Preliminary balanced palinspastic reconstruction of Cenozoic deformation across the Himachal Himalaya (northwestern India)

A. Alexander G. Webb*
Department of Geology and Geophysics, Louisiana State University, Baton Rouge, Louisiana 70803, USA

ABSTRACT

A line-length balanced palinspastic reconstruction across the Himachal Himalaya is presented, highlighting different phases of Himalayan tectonic development: Eocene shortening of the north Indian margin, Early–Middle Miocene emplacement of the crystalline core, and subsequent growth of the range by underplating. The total preserved shortening is 518 km (72%). The reconstruction demonstrates geometric feasibility of crystalline core emplacement via tectonic wedging, i.e., between a south-directed thrust (the Main Central thrust) and a north-directed backthrust (the South Tibet detachment). Crystalline core exposure between these faults occurs ca. 5 Ma in the reconstruction; initial exposure of these crystalline rocks ca. 11 Ma probably occurred in the hinterland within core complexes accommodating east-west extension. After Early–Middle Miocene crystalline core emplacement, ongoing orogenic growth is dominated by underplating processes. Out-of-sequence faulting accomplishes <5% of this shortening; frontal accretion of foreland rocks occurs, but the resulting imbricate fan is largely eroded away. Over the past 3–5 m.y., an antiformal stack of mid-crustal horses and a hinterland-dipping duplex of upper crustal horses develop simultaneously. Minimum total shortening across the western Himalaya (from undeformed foreland to the India-Asia suture) is estimated by adding the new results and results from prior work to the north; an estimate of ~703–773 km of assessed shortening is calculated. However, because large portions of the regional deformation remain unassessed, estimates of ~900–1100 km may more accurately reflect the minimum preserved shortening here. This range is comparable to the ~1350 km of shortening estimated by plate circuit reconstructions for this region. Apparent mismatch between geologic and plate circuit shortening estimates has recently instigated the new Greater India Basin hypothesis for two Cenozoic collisions along Asia's southern margin, but the new results suggest that this mismatch may not exist.

INTRODUCTION

A broad spectrum of growth modes and mechanisms has been proposed to explain portions of the Himalayan tectonic development since closure of the Tethys Ocean ~50 m.y. ago. Ongoing orogenic growth is variably modeled via Mohr-Coulomb critical taper wedge development, or wedge growth by accumulated incremental slip events involving out-of-sequence faulting, frontal accretion, and/or underplating (e.g., Davis et al., 1983; Price, 1988; Dahlen, 1990; Schelling and Arita, 1991; Harrison et al., 1997; Hodges et al., 2001; Avouac, 2003, 2007; Robinson et al., 2003, 2006; Bollinger et al., 2004; Konstantinovskaia and Malavieille, 2005; Wobus et al., 2005; Herman et al., 2010). The emplacement of the orogenic crystalline core is proposed to occur by wedge extrusion (e.g., Burchfiel and Royden, 1985; Grujic et al., 1996; Kohn, 2008), middle and/or lower crustal channel flow coupled to climate-induced, orographically focused denudation (e.g., Nelson et al., 1996; Beaumont et al., 2001, 2004; Hodges et al., 2001), and tectonic wedging (e.g., Yin, 2006; Webb et al., 2007, 2013; Kellett and Grujic, 2012). All these processes are proposed to occur within a single progressive collision, but a new hypothesis posits that the Himalayan orogen records not one, but two Cenozoic collisions with Asia: subduction of a Tethyan-Tibetan microcontinent ca. 50 Ma followed by subduction of India ca. 25–20 Ma (van Hinsbergen et al., 2012).

Viabilities of many tectonic hypotheses have been examined across the central segment of the northwestern Indian Himalaya, i.e., the Himachal Himalaya, because this region has key advantages. First, crystalline core occurrences are highly variable along strike, providing unique exposures of bounding structures (e.g., Thakur and Rawat, 1992; DiPietro and Pogue, 2004; Yin, 2006; Webb et al., 2007). Second, rocks accreted to the orogen here over the past ~10 m.y. display the best-defined and highest-variance stratigraphy along the range, and thus offer the promise of the highest-resolution reconstruction of ongoing deformation processes (e.g., Srikantia and Sharma, 1976; Richards et al., 2005; Célérier et al., 2009a, 2009b; McKenzie et al., 2011). A synthesis of new and existing data (Webb et al., 2011a) indicated that the tectonic development here involves emplacement of the crystalline core via tectonic wedging, succeeded by orogenic growth dominated by underplating, which continues at present.

In this study this tectonic wedging-underplating evolution is modeled via a line-length balanced palinspastic reconstruction. Three primary purposes are accomplished: (1) the cogency of the tectonic wedging-underplating evolutionary model and corresponding interpretation of the current subsurface geology are tested; (2) the geometry of faults and topography during stages of Himalayan orogenesis are explored; and (3) a new minimum shortening estimate is determined. As discussed herein, shortening estimates provide key tests of the new idea that the Himalaya records two Cenozoic collisions along Asia's southern margin, termed the Greater India Basin hypothesis (van Hinsbergen et al., 2012).

HIMALAYAN OROGENESIS

Geologic Framework

The Himalayan orogen marks the collision front between the continents of India and Asia (Fig. 1). It is dominated by a stack of four largely north-dipping, fault-bound units (Heim

*Email: awebb@lsu.edu.

Geosphere; June 2013; v. 9; no. 3; p. 572–587; doi:10.1130/GES00787.1; 5 figures; 1 plate; 1 table.
Received 18 January 2012 ♦ Revision received 15 March 2013 ♦ Accepted 27 March 2013 ♦ Published online 16 May 2013

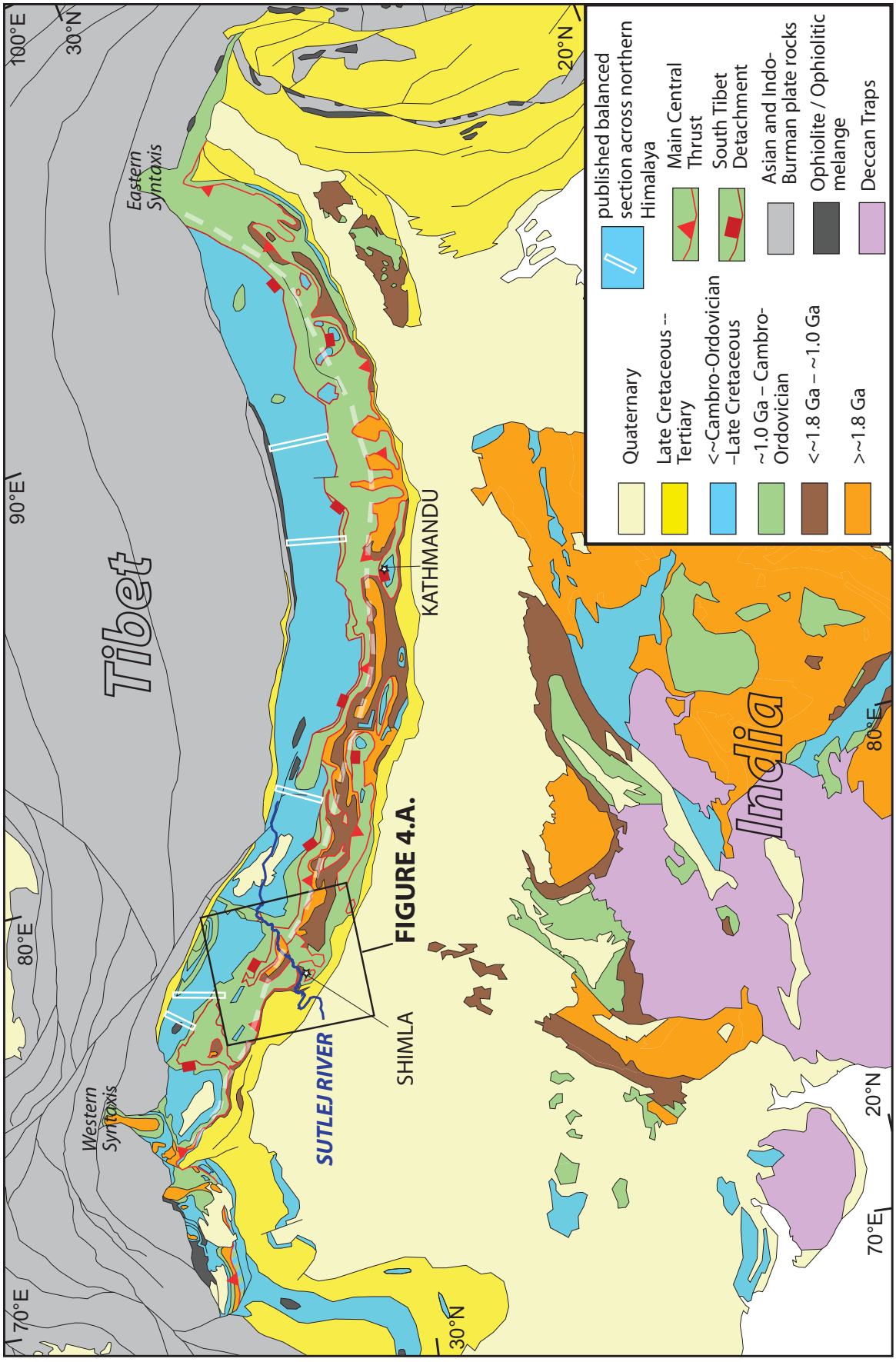

Figure 1. Geological map of the Himalayan orogen (modified from Webb, 2007; Webb et al., 2011a, 2011b). Stratigraphy is depicted on the basis of age, as opposed to tectonic units. Tectonic units are largely defined by the major structures: the pre-Cretaceous Lesser Himalayan Sequence and Cretaceous and younger Sub-Himalayan Sequence underlie the Main Central thrust, the Greater Himalayan Crystalline complex is bound by the Main Central thrust below and the South Tibet detachment above, and the Tethyan Himalayan Sequence occurs above both the Main Central thrust and the South Tibet detachment. Dashed white line indicates the southern margin of a zone of rapid uplift and exhumation (see text discussion, Models for Ongoing Mountain-Building Processes, for an explanation).

and Gansser, 1939; Gansser, 1964; Le Fort, 1975; Hodges, 2000; DeCelles et al., 2001; Yin, 2006). From south to north, these units are (1) the Sub-Himalayan Sequence, foreland basin rocks accreted to the growing orogen; (2) the low-grade Lesser Himalayan Sequence, main locus of orogenic growth via fold-thrust belt development since the Middle Miocene; (3) the high-grade Greater Himalayan Crystalline complex (GHC), bound below and above by the Main Central thrust and South Tibet detachment shear zones, respectively; and (4) the Tethyan Himalayan Sequence (THS), deformed in an Eocene–Oligocene fold-thrust belt (e.g., Heim and Gansser, 1939; Hodges, 2000; Yin, 2006). The Indus-Yarlung suture zone separates these rocks from the Asian plate to the north, and is generally marked by the south-dipping, north-directed Great Counter thrust (Yin et al., 1994, 1999; Murphy et al., 2009; Zhang et al., 2011). The Main Central thrust, South Tibet detachment, and Great Counter thrust were active during the Early to Middle Miocene (Burchfiel and Royden, 1985; Burchfiel et al., 1992; Hodges et al., 1992, 1996; Harrison et al., 2000; Searle, 2010; DeCelles et al., 2011).

Models for the Assembly of the Himalayan Tectonic Units

Models of Himalayan deformation generally feature shortening with lesser lateral spreading, but the juxtaposition of the major tectonic units has also been proposed to involve significant normal faulting along the South Tibet detachment (e.g., Hodges, 2000). Such normal faulting is a key element for two of the three models to explain GHC emplacement, i.e., wedge extrusion (Burchfiel and Royden, 1985) and channel flow coupled to focused denudation (Beaumont et al., 2001), whereas tectonic wedging involves only thrusting (Yin, 2006; Webb et al., 2007). Wedge extrusion shows the GHC as a north-dipping, northward-tapering wedge that extrudes to the south between the Main Central thrust and South Tibet detachment (Fig. 2A). In this model, South Tibet detachment normal faulting may be driven by rotation of principal stresses along the topographic front (Burchfiel and Royden, 1985), or may represent local gravitational collapse within a critical taper orogen (e.g., Burg et al., 1984; Robinson et al., 2006; Kohn, 2008). In channel flow-focused denudation models, the GHC represents partially molten lower and/or middle crust that tunneled southward in the Eocene–Oligocene, driven by the gravitational potential of the high plateau (Fig. 2B). During this period, the South Tibet detachment kinematics match those of a ductile backthrust (e.g., see fig. 3A of Beaumont et al., 2001). In the Early and Middle Miocene, the channel is exhumed between active faults (the Main Central thrust and South Tibet detachment) by erosion across a narrow zone where precipitation is focused by the orography of the topographic front (e.g., Beaumont et al., 2001, 2004; Hodges et al., 2001); thus the South Tibet detachment acts as a normal fault then. In a tectonic wedging model, top-to-the-north motion along the South Tibet detachment represents tens of kilometers of backthrusting, which splays from the Main Central thrust in the Early and Middle Miocene (Fig. 2C). The top-to-the-north South Tibet detachment links to the north-directed Great Counter thrust (Yin et al., 1999).

Models for Ongoing Mountain-Building Processes

The Main Central thrust was the Himalayan sole thrust until ca. 10–15 Ma (e.g., Hodges et al., 1996; Kohn et al., 2004; Tobgay et al., 2012). Shortening since this time incorporates the Lesser Himalayan Sequence and the Sub-Himalayan Sequence into the growing orogen (e.g., DeCelles et al., 2001). Three plane strain models have been proposed to explain the growth of the Himalaya since the Middle Miocene. These models are end members, and thus may work in concert: (1) frontal accretion during forward-propagating thrusting (e.g., Schelling and Arita, 1991); (2) underplating of thrust horses from the downgoing plate to the fold-thrust belt along a ramp of the Himalayan sole thrust (e.g., Robinson et al., 2003; Bollinger et al., 2004, 2006; Murphy, 2007); and (3) out-of-sequence faulting, likewise associated with a ramp of the sole thrust (e.g., Harrison et al., 1997; Wobus et al., 2005) (Fig. 3). Proposed out-of-sequence faults commonly coincide with the northern trace of the Main Central thrust, giving rise to terminology like MCT-I (ca. 10–15 Ma to ca. 1–2 Ma [to recent?] out-of-sequence fault) and MCT-II (sole thrust until ca. 10–15 Ma) (e.g., Upreti, 1999). The MCT-I is commonly correlated with the Munsiari thrust, particularly in the northwestern India Himalaya (e.g., Vannay et al., 2004). In this study the MCT-I is termed the Munsiari thrust, and the MCT-II termed the Main Central thrust.

Debate over ongoing deformation centers on underplating versus out-of-sequence concepts because these models explain a zone of rapid uplift observed across the central band of the Himalaya. The hanging wall of the proposed out-of-sequence fault (i.e., the Munsiari thrust) coincides in map view with the proposed underplating region in an ~20–50-km-wide, orogen-parallel zone coincident with a belt of shallow seismicity and featuring the steepest topography,

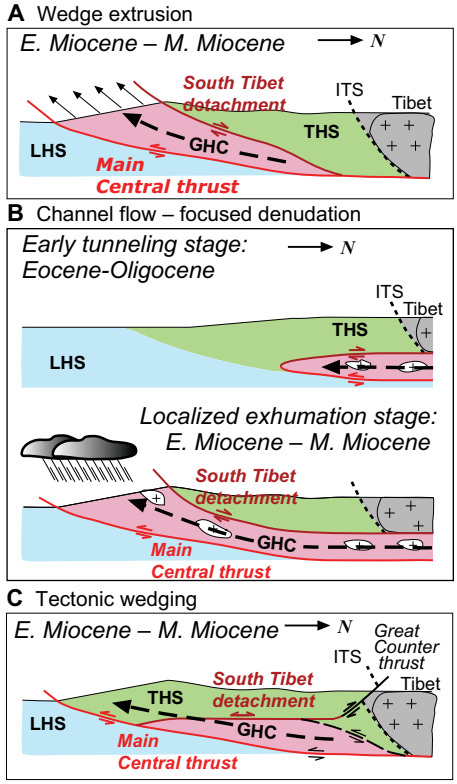

Figure 2. Kinematic models for the emplacement of the Greater Himalayan Crystalline complex (GHC) between the Main Central thrust and the South Tibet detachment (after Webb et al., 2011a). THS—Tethyan Himalayan Sequence; ITS—Indus-Tsangpo suture zone; LHS—Lesser Himalayan Sequence; E—Early; M—Middle. (A) Wedge extrusion and (B) channel flow-focused denudation involve extrusion of the Greater Himalayan Crystalline complex to the surface between two surface-breaching faults (e.g., Burchfiel and Royden, 1985; Beaumont et al., 2001). In contrast, (C) tectonic wedging shows emplacement of this unit at depth, with the two faults merging to the south (e.g., Webb et al., 2007).

highest river incision rates, and highest uplift and exhumation rates along the main length of the arc (e.g., Seeber and Gornitz, 1983; Lave and Avouac, 2001; Wobus et al., 2005). Detailed thermokinematic modeling of thermochronometric data from this zone (and more southern regions) has failed to rule out either underplating or out-of-sequence models (Wobus et al., 2006; Whipp et al., 2007; Herman et al., 2010). Some investigations suggest a late Pliocene increase in erosion and/or exhumation rates, a change that correlates with increased sedimentation in the Indus fan and indicators of an

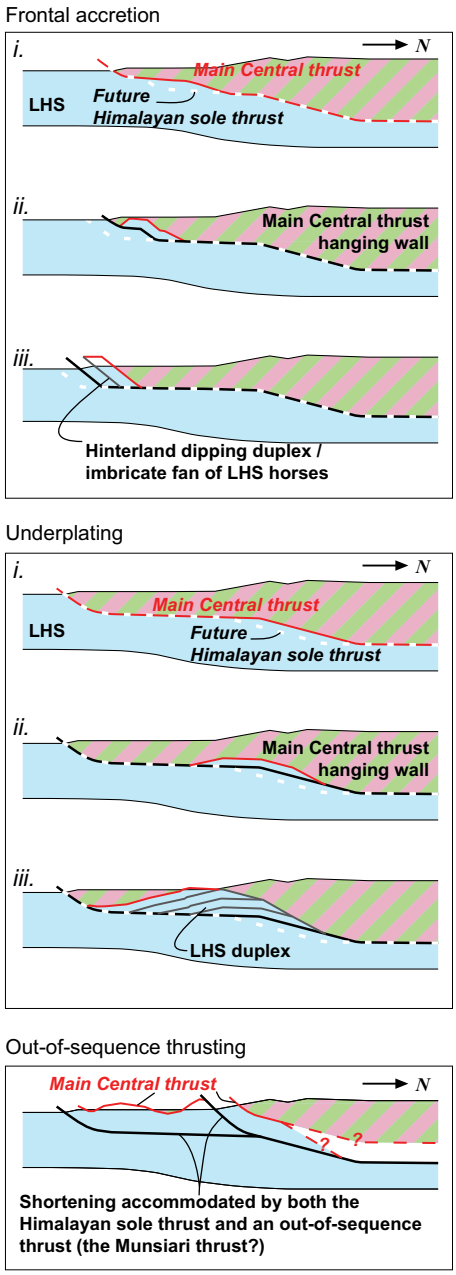

Figure 3. End-member models for the structural evolution of the Main Central thrust footwall and the ongoing growth of the Himalayan orogen. Frontal accretion involves growth of the range by forward propagation of thrusting at the leading edge of the thrust belt (after Schelling and Arita, 1991). LHS—Lesser Himalayan Sequence. Underplating involves incorporation of thrust horses to the growing orogen at depth along the sole thrust (after Bollinger et al., 2004). Active and/or recent out-of-sequence thrusting divides the orogenic hanging wall into two structural plates, both being thrust to the south (after Harrison et al., 1997; Hodges et al., 2001; Thiede et al., 2004).

increasingly wet climate (e.g., Huntington et al., 2006; Clift et al., 2008; Thiede et al., 2009; cf. Herman et al., 2010). Uplift and erosion rates do not correlate consistently with modern precipitation patterns, so a simple relationship between precipitation, erosion, and structural evolution may be precluded (e.g., Burbank et al., 2003; Bookhagen and Burbank, 2006; Blythe et al., 2007; Thiede et al., 2009; cf. Wobus et al., 2003, 2005). Nonetheless, in the absence of a known change in tectonic regime, climate-driven erosion is the most likely cause of increased exhumation rates in the late Pliocene (e.g., Molnar and England, 1990). Analog (sandbox) experiments featuring erosion, multiple décollements, and dominant underplating with lesser frontal accretion are proposed to reproduce the ca. 10–15 Ma to Holocene pattern of Himalayan deformation (Konstantinovskaia and Malavieille, 2005; Avouac, 2007). Such models produce an antiformal stack formed by deep underplating in the hinterland, underlying a zone of maximum exhumation. Toward the foreland, either hinterland-dipping imbricate stacks formed by frontal accretion or duplexes formed by shallow underplating are generated.

Total Himalayan Shortening: Estimates and Implications

India-Asia collisional shortening estimates from plate circuit reconstructions far exceed known geological shortening (Patriat and Achache, 1984; van Hinsbergen et al., 2011a). Plate circuits derived from seafloor magnetic anomaly data show ~2400 and ~3200 km of shortening (at longitudes of western and eastern Himalayan syntaxes, respectively) between stable Eurasia and stable India since a commonly cited collisional age of 50 Ma (Molnar and Tapponnier, 1975; Patriat and Achache, 1984; Dewey et al., 1989; Torsvik et al., 2008; Molnar and Stock, 2009; Cande et al., 2010; Copley et al., 2010; van Hinsbergen et al., 2011b; White and Lister, 2012). Geological shortening estimates since 50 Ma across deformed portions of Asia are only ~1050 km (Pamirs), ~750 km (central Tibet through Mongolia), ~600 km (eastern and northeastern Tibet) (van Hinsbergen et al., 2011a). Similar estimates across deformed portions of India (i.e., the Himalaya) range from 600 to 900 km (see summary of Long et al., 2011a). Resulting shortening deficits range from ~750 km in the west [2400 – (1050 + 600)], ~1150 km in the center [2800 – (750 + 900)], to ~1950 km in the east [3200 – (600 + 650)]. Although the Asian shortening estimates are preliminary and geological shortening estimates are generally minimums, the magnitude of the deficits suggests that large volumes of India may have been subducted below Asia without leaving a shortening record in the Himalaya (Dupont-Nivet et al., 2010; van Hinsbergen et al., 2011a). This possibility led to the recent Greater India Basin hypothesis that the Himalaya records two Cenozoic collisions along Asia's southern margin (van Hinsbergen et al., 2012). In short, this hypothesis posits that a microcontinent dominated by the THS collided with Asia ca. 50 Ma, followed by subduction of a Greater India Basin dominated by oceanic lithosphere. This subduction left little shortening record, and terminated with the collision of the Indian and Asian cratons ca. 25 Ma, with the (currently unidentified) suture zone occurring within the GHC.

GEOLOGY OF THE HIMACHAL HIMALAYA

The geology of the Himachal Himalaya is generally consistent with the stack of four largely north-dipping, fault-bound units described here. A key exception is that from east to west, the immediate Main Central thrust hanging wall changes from an inverted metamorphic sequence consistent with the GHC to a right-way-up metamorphic sequence consistent with the THS (e.g., Thakur, 1998; DiPietro and Pogue, 2004; Leger et al., 2013). Yin (2006) speculated that this transition may result from the merging of the South Tibet detachment and Main Central thrust at the leading edge of the GHC. Field mapping and kinematic analysis confirm this, showing the southernmost South Tibet detachment overturned within the top-to-the-southwest overturned Phojal anticline and intersecting the Main Central thrust (Webb et al., 2007, 2011a). The region also contains the orogen's richest combination of Main Central thrust footwall stratigraphy, structure, and existent thermochronological data (Figs. 1 and 4; Table 1) (e.g., Valdiya, 1980; Webb et al., 2011a). Further details of the regional geology are briefly noted in the following (for a detailed review, see Webb et al., 2011a).

The Sub-Himalayan Sequence here consists of lower shallow-marine strata and upper continental deposits. The Lesser Himalayan Sequence is divided into four units: (1) the Neoproterozoic–Cambrian Outer Lesser Himalayan Sequence, (2) the Paleoproterozoic–Neoproterozoic Damtha and Deoban Groups, (3) the Paleoproterozoic Berinag Group, and (4) the Paleoproterozoic Munsiari Group. All Lesser Himalayan Sequence units are dominated by metasiliciclastic and/or siliciclastic rocks except the Deoban Group, which is composed largely of carbonates, and the Munsiari Group, which contains ca. 1.85 Ga orthogneiss and paragneiss. A laterally discontinuous strip of gra-

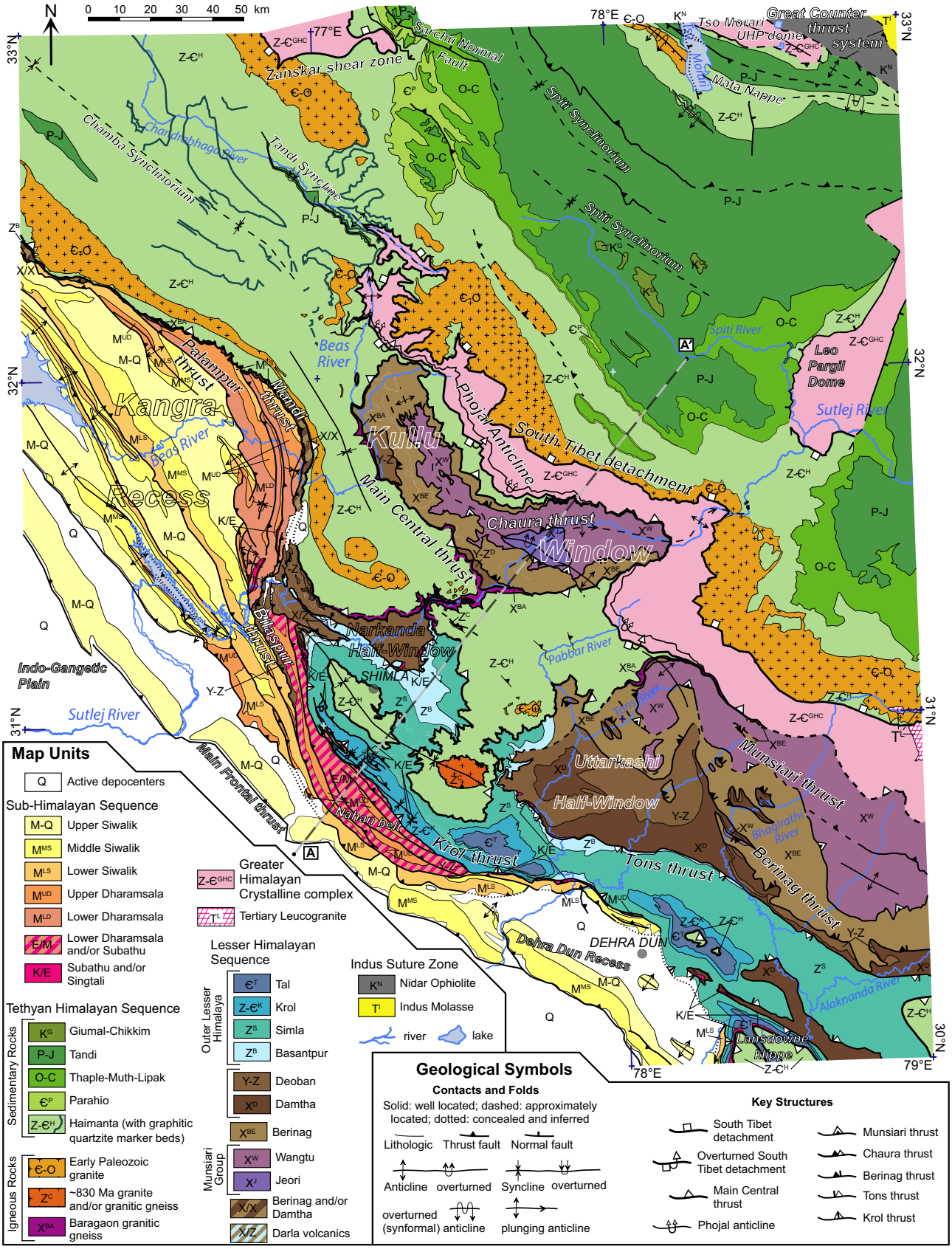

Figure 4 (*on this and following page*). **(A) Geological map of the Himachal Himalaya (modified from Webb et al., 2011a). Unit descriptions are in Table 1.**

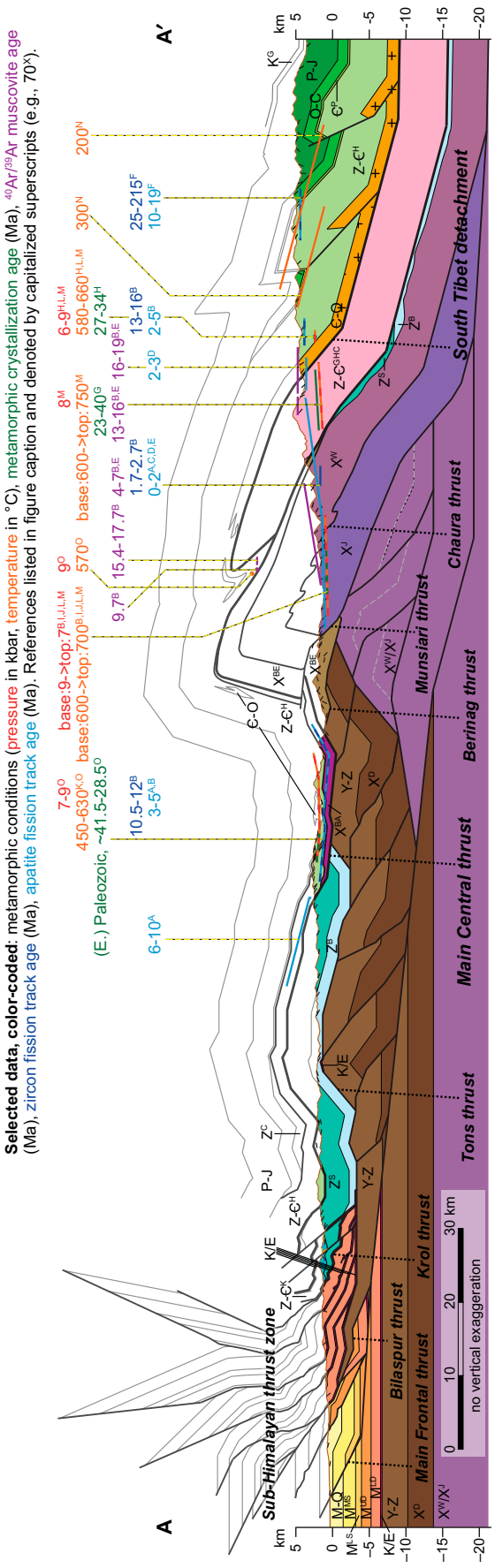

Figure 4 (*continued*). (B) Cross section of the Himachal Himalaya (modified from Webb et al., 2011a). Section is drawn along line A-A′ of A. MCT—Main Central thrust, STD—South Tibet detachment. Brown curve represents Earth's surface; short black lines along Earth's surface represent bedding and/or foliation attitudes. All faults are top-to-the-southwest with the exception of the STD, which displays records of both top-to-the-southwest and top-to-the-northeast motion. References for analytical data are superscripts: A—Thiede et al. (2009); B—Vannay et al. (2004); C—Jain et al. (2000); D—Thiede et al. (2004); E—Thiede et al. (2005); F—Schlup et al. (2011); G—E. Catlos, 2004, personal commun.; H—Chambers et al. (2009); I—Chambers et al. (2008); J—Caddick et al. (2007); K—Gregory (2004); L—Vannay and Grasemann (1998); M—Vannay et al. (1999); N—Wiesmayr and Grasemann (2002); O—Webb et al. (2011a).

nitic gneisses (Baragaon gneiss) lithologically correlative to the Munsiari Group occurs within the Main Central thrust zone. Protoliths of the GHC and lower THS (Haimanta Group) are dominated by Neoproterozoic–Cambrian siliciclastics correlative to the Outer Lesser Himalayan Sequence and contain lesser volumes of early Paleozoic granite. Upper portions of the THS display a well-characterized Paleozoic–Mesozoic sequence, with much of the Paleozoic sequence missing to the south such that erosional remnants of Permian–Triassic rocks directly overlie the Haimanta Group (e.g., Frank et al., 1995; Vannay and Steck, 1995).

The GHC displays an inverted metamorphic field gradient from garnet-staurolite–bearing rocks to migmatitic rocks near the top. The Lesser Himalayan Sequence and THS are largely anchizone to greenschist facies, with grade increasing in both units toward the GHC such that the regional temperature increase into the GHC across the bounding faults is generally <100 °C (e.g., Vannay and Grasemann, 1998; Vannay et al., 1999; Caddick et al., 2007; Célérier et al., 2009a, 2009b; Chambers et al., 2008, 2009; Leger et al., 2013).

Major fault zones and fault systems of the Main Central thrust footwall are southwest-directed thrusts. From southwest to northeast, these are (1) the Main Frontal thrust, (2) the Sub-Himalayan thrust zone, (3) the Bilaspur-Palampur thrust system, (4) the Krol-Mandi thrust system, (5) the Tons thrust, (6) the Berinag thrust, (7) the Munsiari thrust, and (8) the Chaura thrust. Several large structural culminations are also exposed in the map area due to folding of major thrusts, i.e., the Narkanda half window, the Uttarkashi half window, and the Kullu window. The structural geometry of the eastern Kullu window is well correlated with the trace of the Sutlej River, as recorded by a river anticline (Oberlander, 1985; Montgomery and Stolar, 2006). In the west, the Kangra recess is the largest recess along the main Himalayan arc (e.g., Powers et al., 1998). The Main Central thrust and South Tibet detachment are both characterized by thick, dominantly ductile shear zones, 1–2 and 0.3–0.6 km thick, respectively. Deformation within the Main Central thrust zone is uniformly southwest-directed, whereas the South Tibet detachment records evidence of alternating northeast- and southwest-directed shear (e.g., Jain et al., 1999). Every unit in the region records internal shortening: outcrop observations suggest that internal shortening is typically no less than ~10% and locally exceeds 50% (e.g., Vannay et al., 2004; Webb et al., 2011a).

Kinematic models of ongoing deformation across the study area are based largely upon

TABLE 1. TECTONOSTRATIGRAPHY OF THE HIMACHAL HIMALAYA

Unit name (alternative name)	Lithologic description	Thickness (m)	Age constraints	Nd, Sr isotopic constraints*
Himalayan Foreland**				
Upper Siwalik Fm†	ss, congl	~1700–2300	deposition 7 Ma–Pleistocene: MS§	N.D.
Middle Siwalik Fm	ss with minor slts, sh, congl	~1300–2000	deposition 11–7 Ma: MS§	N.D.
Lower Siwalik Fm	slts with minor ss, sh	~700–1300	deposition 13–11 Ma: MS§	N.D.
Upper Dharamsala Fm (Kasauli)	gray ss, minor sh (fluvial and/or alluvial)	~1000–1300	deposition 16.5–13 Ma: MS, cf. detrital mica§	N.D.
Lower Dharamsala Fm (Dagshai)	ss, slts, sh, caliche (fluvial and/or alluvial)	to 1300	deposition 20–16.5 Ma: MS, cf. detrital mica§	N.D.
Subathu Fm	ls, sh, minor fine-grained ss (shallow marine)	to 200	latest Paleocene–Middle Eocene: fossils	N.D.
Singtali Fm	ls, minor quartz arenite (shallow marine)	~50, discontinuous	Late Cretaceous–Paleocene: fossils††	N.D.
Lesser Himalayan Sequence: Outer Lesser Himalaya				
Tal Fm	ss, slts	~500	Lower Cambrian: trilobites, Re-Os isochron	≤NPt*
Krol Gp	dl, ls with minor sh, slts	~1500–2200	ca. 590–543 Ma: fossils, $\delta^{13}C$ shift	≤NPt
Shimla Gp (Chandpur, Nagthat, Blaini)	sh (minor slate), slts, ss, with minor gw, tillite, congl	~3800–4100	younger than ca. 620 Ma: detrital U-Pb zrc; stratigraphically below Krol Gp	≤NPt
Basantpur Fm (Mandhali)	interbedded ls, slts, sh (minor slate)	>~300–640	839 ± 138 Ma: Re-Os isochron, Neoproterozic strom	≤NPt
Lesser Himalayan Sequence: Parautochthon				
Deoban Gp (Shali)	dl, ls with minor sh, chert, ss	>~3000	≥2 levels, lower: (latest Paleozoic?) Mesoproterozic, upper: Neoproterozic strom and other fossils	≥MPt*
Damtha Gp (Sundarnagar: Chakrata, lower member; Rautgara, upper member)	gw, slts, slate succeeded by qtzt, sl, basic sills and dikes	>~2900	≥Paleoproterozic, stratigraphically below Deoban Gp	N.D.
Lesser Himalayan Sequence: Berinag thrust hanging-wall rocks				
Berinag Gp (Rampur, Manikaran)	greenschist facies sericitic quartz-arenite, metabasalt (sills, dikes, flows), minor sl	>~1000	younger than ca. 1.85–1.8 Ga: detrital U-Pb zrc, U-Pb zrc from metabasalt	qtzt: ≥MPt metabasalt: ≤NPt
Lesser Himalayan Sequence: Munsiari Group				
Wangtu gneiss (Bandal)	dominantly granitic augen gneiss	>~2000	younger than ca. 1.85 Ga: Rb-Sr whole rock, U-Pb zrc	≥MPt
Jeori metasedimentary rocks	paragneiss, mica schist, minor metabasite, qtzt, granitic gneiss	unknown	some layers <~1.9 Ga, other layers >~2068 Ma: detrital U-Pb zrc, igneous U-Pb zrc	≥MPt
Felsic pegmatite (crosscuts Wangtu gneiss foliation)		to ~4-m-thick dikes	younger than ca. 8-6 Ma: U-Pb zrc, Th-Pb monazite	N.D.
Greater Himalayan Crystalline complex	paragneiss, schist, orthogneiss	~4500–8000	some layers younger than ca. 850 Ma: detrital zrc, 495 Ma orthogneiss: Rb/Sr	≤NPt
Leucogranite		up to hundreds of meters thick	younger than ca. 27–20 Ma: U-Pb monazite, uraninite, Th-Pb monazite	N.D.
Tethyan Himalayan Sequence: Sedimentary rocks				
Giumal-Chikkim succession	ss, black sh, ls	~350	Cretaceous: fossils	N.D.
Tandi Gp	carbonate, sh, slts, qtzt	>~1920	Permian–Jurassic: fossils	N.D.
Thaple-Muth-Lipak succession	sh, slts, qtzt, quartz-arenite, carbonate, congl	~1650	Ordovician–Carboniferous: fossils	N.D.
Parahio Fm	ss, sh (siliciclastic deltaic)	~700	uppermost-lower Cambrian–middle-middle Cambrian: fossils	N.D.
Haimanta Gp	phyllite, schist, garnet schist, graphitic schist, psammitic schist, minor carbonate, minor metabasalt	>~6250	younger than ca. 550 Ma–early Cambrian: trilobites, crosscutting igneous ages, detrital U-Pb zrc	≤NPt
Tethyan Himalayan Sequence: Igneous rocks				
Early Paleozoic granitoids	granite, minor mafic enclaves, minor aplite, locally gneissic	to at least ~2000	Cambrian–Ordovician: Rb-Sr whole rock, U-Pb zrc	≤NPt
ca. 830 Ma (Chaur–Black Mountain) granite	granite, granitic gneiss	to ~3000	ca. 830 Ma: U-Pb zrc	N.D.
Baragaon granitic gneiss	mylonitic granitoid gneiss	to ~1100	ca. 1.85 Ga: Rb-Sr whole rock, U-Pb zrc	≥MPt
Indus suture zone				
Nidar Ophiolite	ultramafics, gabbros, pillow basalts	~2100–2700	140.5 ± 5.3 Ma: Sm-Nd (plagioclase-clinopyroxene)	N.D.
Indus molasse	sh, slts, ss, congl	unknown	Early Eocene	N.D.

Note: Modified from Webb et al. (2011a).

*Himalayan pre-Cenozoic rocks plot in two largely distinct groups in Nd and Sr isotopic space. These groups can be distinguished by age: Mesoproterozoic and older rocks yield $\varepsilon_{Nd}(500) < \sim -14$ and a broad range of $^{87}Sr/^{86}Sr$ (500) values (this group is abbreviated as "≥MPt"), whereas Neoproterozoic and younger rocks yield $\varepsilon_{Nd}(500) > \sim -14$ and a narrow range of $^{87}Sr/^{86}Sr$ (500) values ("≤NPt"). (Corresponding data plots are shown in Supplemental File 2 of Webb et al., 2011a.)

†Additional abbreviations: Fm—Formation, Gp—Group, congl—conglomerate, ss—sandstone, slts—siltstone, sh—shale, gw—graywacke, ls—limestone, dl—dolomite, qtzt—quartzite, N.D.—not determined, MS—magnetostratigraphy, zrc—zircon, strom—stromatolites.

§The age estimates for the Miocene and younger Himalayan foreland rocks largely depend on magnetostratigraphic correlation. However, the youngest $^{40}Ar/^{39}Ar$ age of detrital white micas, which record the time at which the mica cooled below ~370 °C, provide a maximum age of deposition. Detrital mica ages of ca. 22 Ma at the base of the Lower Dharamsala, and ca. 16 Ma in the Upper Dharamsala, are only consistent with the proposed magnetostratigraphic ages if extraordinary cooling rates are invoked (see Yin, 2006). The youngest white mica ages obtained from Himalayan bedrock are older than 4 Ma (Célérier et al., 2009b), so using ~4 m.y. as a minimum lag time between the cooling age and depositional age suggests that the magnetostratigraphic ages for the Lower and Upper Dharamsala are at least ~2 m.y. too old. Adjusting the ages of these units may also affect interpreted ages of the Siwalik strata.

**According to the Powers et al. (1998) model, the Himalayan sole thrust occurs along the onlapping depositional contact of the Tertiary foreland basin over the Vindhyan Group. In this scheme, the Lower Dharamsala and Subathu pinch out along the onlapping depositional contact, and thus have 0 thickness at the pinch out. The exposed sections of these units have thicknesses tending toward the upper thickness values given.

††Valdiya (1980) noted that the "lower Singtali" may be equivalent to a late Paleozoic–early Mesozoic sedimentary sequence termed the Gondwana unit.

structural transects and thermal and/or thermochronological data across the northern Lesser Himalayan Sequence and the Main Central thrust hanging wall. Models alternately show (1) a dominant out-of-sequence thrust with synchronous, structurally higher normal faulting (e.g., Thiede et al., 2004, 2005, 2009; Vannay et al., 2004) or (2) upper and/or middle crustal underplating (Srivastava and Mitra, 1994; Célérier et al., 2009b). Thermochronological investigations across the region confirm the presence of the zone of rapid uplift and exhumation (Fig. 4B; also see fig. 7 of Thiede et al., 2009) (e.g., Jain et al., 2000; Thiede et al., 2004, 2005, 2009; Vannay et al., 2004; Schlup et al., 2011), as documented elsewhere along the range (Fig. 1). Exhumation rates across this zone have been ~1–3 mm/yr for the past ~13 m.y., although the location of the northern margin has fluctuated (Thiede et al., 2009). Immediately north and south of this zone, exhumation rates are <1 mm/yr over this period (Thiede et al., 2009).

BALANCED PALINSPASTIC RECONSTRUCTION

To assess the Cenozoic kinematic history, a balanced palinspastic reconstruction (Plate 1) of the deformed cross section (Fig. 4) presented in Webb et al. (2011a) was made. The section extends from the Indo-Gangetic Plain, across the Kullu window, and into the THS fold-thrust belt. Adjacent balanced cross sections across the Sub-Himalayan Sequence (Powers et al., 1998) and THS (Wiesmayr and Grasemann, 2002) were simplified, but otherwise incorporated without significant alteration. Similar balanced cross sections across the Lesser Himalayan Sequence by Srivastava and Mitra (1994) were largely disregarded because updated stratigraphic interpretations limit their utility. Specifically, Srivastava and Mitra (1994) posited correlation of the Berinag and Deoban Groups with the Outer Lesser Himalayan Sequence, but subsequent work demonstrated significant age differences (e.g., Ahmad et al., 2000; Richards et al., 2005; McKenzie et al., 2011; Webb et al., 2011a).

Restored time steps were constructed by progressively "undeforming" the deformed section using a combination of 2D Move software (from Midland Valley Exploration Ltd.) and standard vector graphics software (Adobe Illustrator). A kink-band approach was employed: layer-parallel simple shear was used to fit restored fold limbs after unfolding. Primary goals were to minimize shortening and to model a progressive deformation pattern consistent with existing geometric and thermochronologic constraints (summarized in Webb et al., 2011a). Approximate periods of 5 restored time steps are pre–45 Ma, 23 Ma, 14 Ma, 5.4 Ma, and 1.9 Ma (Plates 1B–1F, respectively). The time estimates of 5.4 Ma and 1.9 Ma for time steps E and F were determined by measuring shortening estimates for each section (~101 km and ~35 km, respectively) and using the geodetic shortening rate across this segment of the Himalaya of 18.8 mm/yr (Jade et al., 2004) to calculate an age. A similar calculation for the section of Plate 1D (~319 km shortening) produces an age of ca. 17 Ma, but a ca. 14 Ma age is assigned because of its slightly better fit to the cooling history of the southern Main Central thrust hanging wall and the possible decrease in the shortening rate over time (cf. Molnar and Stock, 2009). Ages assigned to time steps B and C are based not on shortening rate considerations, but rather on the thermochronologic data sets across restored units. The section preserves very few constraints on the shortening and overall kinematic evolution from the latest Eocene to the Early Miocene.

The reconstruction is first order at best; it is line-length balanced in a region where outcrop analyses of most units commonly show significant internal shortening. Furthermore, plane strain is assumed, even though the section clearly underwent 3D deformation (e.g., river anticline development along the Sutlej River; Fig. 4A; see also Montgomery and Stolar, 2006). Nonetheless it satisfies current knowledge of the first-order structural geometry, stratigraphy, and pressure-temperature-time constraints, and it provides basic shortening estimates. Restored stages and associated deformation are discussed in the following.

Configuration Prior to Shortening (> 45 Ma)

A schematic model of the pre-Cenozoic stratigraphy of the study area is presented in Plate 1A. This model was discussed in detail in Webb et al. (2011a). Our restored geometry (Plate 1B) is a close match to the schematic model (Plate 1A), with minor changes that allow minimization of shortening. Undeformed positions of the Outer Lesser Himalayan Sequence and Berinag Group are changed slightly; the former dips gently to the north, and the latter represents an isolated basin. The restored length of ~720 km yields a minimum estimate of Cenozoic shortening of 518 km (72%).

Dashed red lines shown across the restored geometry (Plate 1B) highlight fault traces that were active between ca. 45 Ma and ca. 23 Ma, i.e., prior to time step C. This device is used to clarify where faults develop in the period following each restored time step.

Restoration ca. 23 Ma

The only distinction between the fully restored geometry (Plate 1B) and the ca. 23 Ma time step (Plate 1C) is the northern THS fold-thrust belt (drawn after Wiesmayr and Grasemann, 2002). Approximately 11 km of shortening are accommodated within the preserved THS fold-thrust belt along the line of section. The paleogeography and cooling history are sufficiently uncertain that we do not show an inferred ground surface. Outcrop observations and Th-Pb geochronology of monazite included in garnet indicates that additional THS shortening occurred farther south during the 45–23 Ma interval (Webb et al., 2011a), but very limited preservation of the southern THS precludes restoration. Approximately 200 km to the northwest of the line of section, along-strike equivalent THS rocks are involved in a fold-thrust belt (e.g., Frank et al., 1995), so it is likely that a similar deformation belt was eroded here.

Restoration ca. 14 Ma

Deformation between the 23 Ma and 14 Ma time steps is dominated by the emplacement of the Main Central thrust sheet (Plate 1D). In this interval the GHC, THS, and Baragaon gneiss are thrust over the Outer Lesser Himalayan Sequence and Berinag Group. All of these rocks move to the southwest relative to the Main Central thrust footwall. During this deformation, tectonic wedging of the GHC also occurs: the overthrusting Main Central thrust hanging wall is broken into two parts, and the Baragaon gneiss and THS rocks move northward relative to the underthrusting GHC. This motion is accommodated by the South Tibet detachment, and followed by the development of the Phojal anticline. This fold warps the southwestern end of the South Tibet detachment but does not appear to deform the Main Central thrust, so it is interpreted as a detachment fold along the latter fault. With the exception of folding of the Phojal anticline, the GHC is treated as an undeformed layer. The restoration does not represent or quantify the significant internal deformation of this unit (cf. Jain and Manickavasagam, 1993; Corrie and Kohn, 2011).

The emplacement of the Main Central thrust sheet and tectonic wedging of the GHC require ~181 km of shortening. Thermochronological data across the northern portion of the line of section are sufficient to infer the position of the ground surface at this time. Units that remain deeply buried at this time include the Baragaon gneiss, the southern THS hanging wall, the leading edge of the GHC, the Munsiari Group (see Fig. 4B and references therein), and the Berinag Group (as constrained to the southeast by

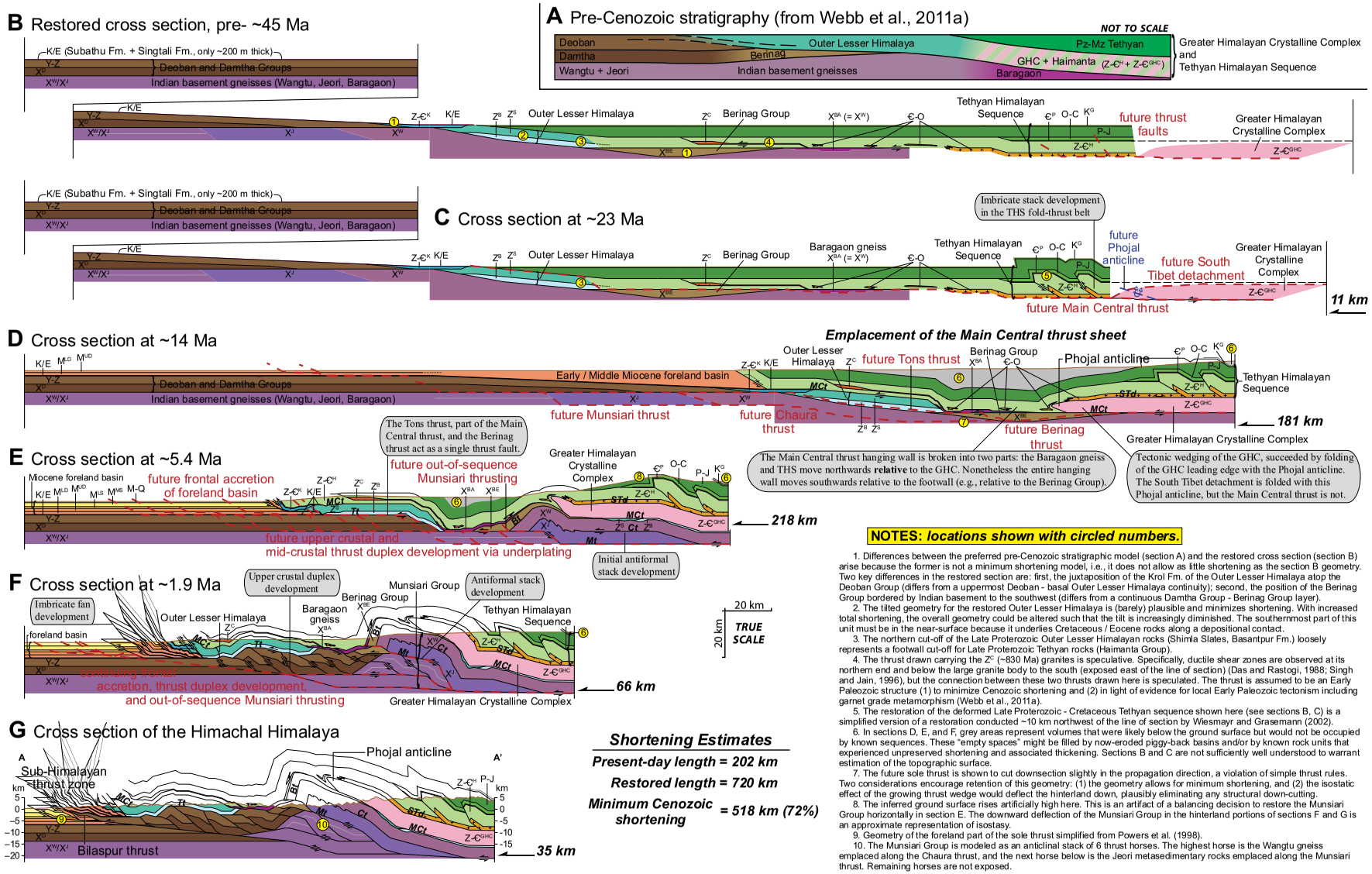

Plate 1. Sequential cross-section restoration across the Himachal Himalaya along line A–A′ (see Fig. 4). Abbreviations: Bt—Berinag thrust, Ct—Chaura thrust, GHC—Greater Himalayan Crystalline complex, MCt—Main Central thrust, Mt—Munsiari thrust, STd—South Tibet detachment, THS—Tethyan Himalayan Sequence, Tt—Tons thrust. (A) Schematic model of pre-Cenozoic stratigraphy (from Webb et al., 2011a). (B–G) Palinspastic reconstructions. (B) Initial configuration prior to significant Cenozoic shortening in the region. Differences between this model and the model in A allow minimum shortening (see note 1). (C) Development of the Tethyan fold and thrust belt. (D) Emplacement of the Main Central thrust hanging wall, synchronous with motion along the South Tibet detachment. Late top-to-the-southwest shear deforms the Main Central thrust hanging wall, creating the Phojal anticline. (E) Emplacement of Tons thrust and Berinag thrust hanging walls, initial development of antiformal stack of Indian basement (Munsiari Group). (F) Development of upper and middle crustal duplexes through underplating concurrent with frontal accretion of foreland basin strata and out-of-sequence faulting along the Munsiari thrust. (G) Last stage in the development of the current architecture involves continued underplating, frontal accretion, and out-of-sequence faulting. See Figure 5 for a detailed reconstruction of the Bilaspur thrust sheet emplacement. Abbreviations as in Figure 4. To view the full-sized (11 × 17) PDF file of Plate 1, please visit http://dx.doi.org/10.1130/GES00787.S1 or the full-text article on www.gsapubs.org.

Célérier et al., 2009b). Some unaccounted material must have overlain these units (see note 6 in Plate 1). Likely candidates are shortened, thickened THS rocks and/or intermontane basin fill. Similarly, most of the potentially large Early–Middle Miocene foreland basin is now removed via erosion.

Restoration ca. 5.4 Ma

From ca. 14 to 5.4 Ma, deformation propagates downsection (Plate 1E). The first underplated slices are the Berinag Group (along the Berinag thrust) and the Outer Lesser Himalayan Sequence (along the Tons thrust). In order to minimize shortening, the Berinag and Tons thrusts are interpreted as the same fault, connected here by continued slip along a small portion of the Main Central thrust. Munsiari Group thrust horses defined by the basal Chaura and Munsiari thrusts are shown as the next accreted slices. Note that the predeformation traces of the Berinag and Tons thrusts slice through the Berinag Group and Outer Lesser Himalayan Sequence, respectively (this is not geometrically required, but to exclude such cutting strains geologic plausibility) (Plate 1D). Therefore, the thrust horse underlain by the Chaura thrust is interpreted to contain thin fragments of the Outer Lesser Himalayan Sequence and the Berinag Group. Along the line of section, these interpreted fragments remain buried. To the southwest slip is locally concentrated along a single thrust that cuts upsection across the Deoban and Damtha Groups. The hanging-wall cutoff of these Deoban and Damtha rocks is interpreted to be completely erosionally removed by ca. 5.4 Ma.

Approximately 218 km of shortening is absorbed during emplacement of the Berinag, Chaura, and Tons thrust hanging walls and initial motion along the Munsiari thrust. The restored ground surface (based on thermochronometric results summarized in Fig. 4B) indicates dramatic erosive removal of material at the leading edge of the fold-thrust belt and only minor erosive loss to the north. The bulk of the unaccounted material above known units is removed by this time (see note 6 in Plate 1). The model section also displays deposition of most of the preserved Sub-Himalayan Sequence by this time. With reference to models for emplacement of the GHC (see Fig. 2), it is noteworthy that the GHC may not be exposed along the line of section at ca. 5.4 Ma.

Restoration ca. 1.9 Ma

In the model interval between ca. 5.4 and 1.9 Ma, a leading imbricate fan, an upper crustal duplex, and a middle crustal antiformal stack develop (Plate 1F). These structural packages deform the Sub-Himalayan Sequence, Deoban and Damtha Groups, and Munsiari Groups, respectively. The lengths of thrust sheets decrease significantly (although for the frontal accretion of the imbricate fan there are no older analogous structures preserved to provide a basis for comparison). Out-of-sequence faulting along the Munsiari thrust is shown to cut upsection across the Berinag and Main Central thrusts.

The structural development from ca. 5.4 Ma to ca. 1.9 Ma involves ~66 km of shortening. The inferred ground surface ca. 1.9 Ma is largely similar to the modern exposure level, excepting locally high exhumation at the range front and above the antiformal stack. The modeled uplift history of the antiformal stack, with most currently exposed units coming from mid-crustal depths (~10–15 km) over the past ~5 m.y., is a good match with thermochronological results of ca. 1–2 Ma apatite fission track and ca. 5 Ma $^{40}Ar/^{39}Ar$ muscovite ages for these rocks along the Sutlej River (Jain et al., 2000; Thiede et al., 2004, 2005, 2009; Vannay et al., 2004). Vannay et al. (2004) noted (1) late top-to-the-east shear bands in Main Central thrust zone along the Sutlej River at the east end of the Kullu window; (2) a top-to-the-east, east-dipping cataclastic fault zone in the basal GHC along the Sutlej River; and (3) a sharp break in thermochronological ages, across the Main Central thrust here, from the ca. 5 Ma $^{40}Ar/^{39}Ar$ muscovite ages in the Munsiari Group to ca. 15–18 Ma ages in the GHC. They interpret these results to indicate that a late normal fault cuts along the Main Central thrust and accommodates the Miocene–Holocene exhumation of the Munsiari Group along the Munsiari thrust. The present reconstruction offers an alternative interpretation: the shearing may result from minor layer-parallel slip accommodating small space issues during the growth of a Munsiari anticlinal stack, for which the Main Central thrust may act as a roof thrust. The age gradient across the Main Central thrust would reflect the deeper, hotter structural position of the Munsiari Group prior to ca. 5 Ma. That is, the Main Central thrust would be subhorizontal during the Miocene. After GHC cooling in the Early–Middle Miocene, the approximate isotherm marking Ar closure in muscovite would coincide roughly with the Main Central thrust until after the Munsiari uplift had begun.

The Munsiari Group is modeled as an anticlinal stack of six thrust horses. This stack requires no fewer than four horses. Modeling with fewer horses results in less shortening of the Munsiari Group. Decreased shortening presents difficulties for initiation of Munsiari Group uplift ca. 7–10 Ma (e.g., Caddick et al., 2007); this is because with much less shortening and a minimum shortening rate of ~18.8 mm/yr [i.e., the modern global positioning system (GPS) determined shortening rate from Jade et al., 2004), the Munsiari uplift would be required to have initiated more recently.

Late Deformation to Deformed Cross Section

Deformation from ca. 1.9 Ma to the present involves continued frontal accretion and underplating (Fig. 4B and Plate 1G). Development of the Deoban-Damtha duplex involves cutting upsection along a shallow ramp. This satisfies requirements of (1) a thin slice of Deoban present along the Bilaspur thrust (Fig. 4) and (2) the dip of the active sole thrust as constrained by balancing, seismic reflection, and boreholes across the Dehra Dun and Kangra recesses (Fig. 4) (Powers et al., 1998).

Approximately 35 km of shortening are accommodated from ca. 1.9 Ma to the present. Restoration of the Bilaspur thrust involves space issues related to the emplacement of the aforementioned thin layer of Deoban rocks within the Sub-Himalayan thrust zone. These were resolved with a kinematic evolution involving out-of-sequence thrusting, as shown in Figure 5. The overall geometry of the Sub-Himalayan thrust zone in the Bilaspur thrust hanging wall is poorly understood; a duplex model may be an alternative. Out-of-sequence faulting is also shown along the Munsiari thrust, with as much as 8 km of slip from ca. 4–5 Ma to the present.

DISCUSSION

The balanced palinspastic reconstruction highlights different phases of Himalayan tectonic development, showing (1) a small fraction of Eocene shortening of the THS, (2) Early–Middle Miocene emplacement of the Main Central thrust sheet with tectonic wedging of the GHC, (3) Middle–Late Miocene underplating of ~50–150-km-long thrust sheets, and (4) Pliocene–Holocene frontal accretion and formation of 2 duplexes dominated by ~10–25-km-long horses. In general, structural preservation decreases with increasing age. Likewise, shortening estimates for various periods are increasingly poorly constrained with increasing age. The total preserved shortening is 518 km and 72%. The nonuniqueness of reconstruction efforts, implications for tectonic models, and the shortening budget are discussed in the following.

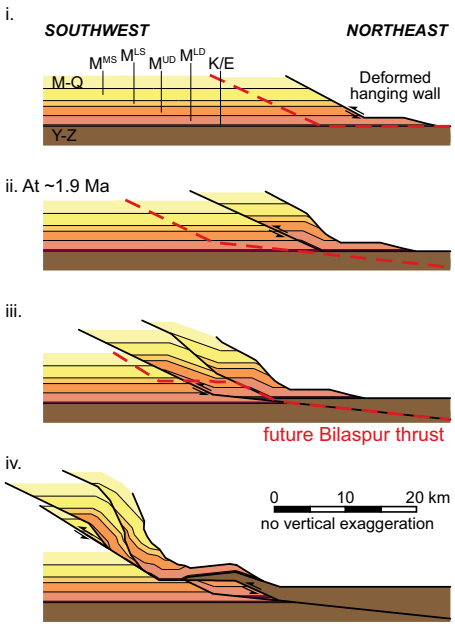

Figure 5. Structural evolution of the Bilaspur thrust along section line A–A′. First phase (i) geometry is during the development of the Sub-Himalayan thrust zone, with the undisplayed deformed hanging wall to the northeast. Southwestward thrust propagation along the same décollement at the top of the Proterozoic Deoban rocks continues until ca. 1.9 Ma (ii). After ca. 1.9 Ma (iii), the basal fault of the forward-propagating system migrates downsection to the middle of the Proterozoic Deoban rocks. A segment of the Bilaspur thrust reactivates an earlier thrust as an out-of sequence thrust, then cuts southwestward and ramps up along an in-sequence segment (iv). Abbreviations as in Figure 4.

Nonuniqueness of Balanced Palinspastic Reconstruction

Line-length balanced palinspastic reconstruction offers a nonunique model of the deformation process. The synoptic view is reasonably well constrained, but any one portion of the reconstructed geology may not be well represented. For example, along the restored section the Deoban and Damtha Groups are shown within a simple hinterland-dipping duplex consisting of eight discrete horses. However, field observations of 1–300-m-scale brittle contractional structures across much of this unit (e.g., Srikantia and Sharma, 1976; Webb et al., 2011a) suggest that a mushwad duplex interpretation (e.g., Thomas, 2001; Cook and Thomas, 2010) is equally valid. Furthermore, the same geometries can be restored by different kinematics. For example, the northern limit of the Tons thrust may terminate along the Main Central thrust (as shown in Fig. 4B; also see fig. 16 of Webb et al., 2011a). The reconstruction (Plate 1) suggests that this relationship develops by underplating of the Tons thrust hanging wall to the Main Central thrust hanging wall, but it could result from out-of-sequence faulting along the Main Central thrust after Tons thrust motion. The line-length balancing approach minimizes shortening by ignoring intraunit deformation. The impact of this neglect on Himalayan sections is debated: recent work suggests that it could be insignificant across much of the Lesser Himalayan Sequence (cf. Yin et al., 2010 and Long et al., 2011b).

Emplacement of the Greater Himalayan Crystalline Complex

Three models are widely discussed to explain the emplacement of the GHC (Fig. 2). The deformed cross section limits reconstruction options to only the tectonic wedging model, because the leading edge of the GHC is only recently eroded along the line of section. Wedge extrusion and channel flow-focused denudation models both feature emplacement of the GHC at the surface during the Early–Middle Miocene. The ca. 23–15 Ma GHC surface exposure inherent in this prediction requires continuous exposure of the GHC along the entire arc of the orogen, except where broken by Late Miocene–Holocene deformation (e.g., south of Gurla Mandhata in western Nepal; Murphy and Copeland, 2005). Detailed field mapping documents THS stratigraphy separating GHC exposures at southern Zanskar (~33°N, 77°E) and at the uppermost Beas River Valley (~32°20′N, 77°10′E) (Fig. 4A) (e.g., Frank et al., 1995; Fuchs and Linner, 1995; Vannay and Steck, 1995), precluding GHC continuity.

The palinspastic reconstruction demonstrates the geometric feasibility of GHC emplacement via tectonic wedging by illustrating the southern parts of this process. Top-to-the-northeast slip along the South Tibet detachment requires only tens of kilometers of motion, consistent with the matching protoliths and moderate metamorphic grade transition across the structure. This top-to-the-northeast motion would be expressed at the surface by the coeval Great Counter thrust to the northeast (e.g., Yin, 2006). Therefore, the South Tibet detachment may not significantly alter the kinematic and thermal pattern imposed by southwest-directed thrusting along the Main Central thrust, but rather accomplish relatively modest contraction of the hanging wall (Yin, 2006; Webb et al., 2007).

The proposed relative motion of the GHC and surrounding units is directly analogous to the Eocene–Oligocene tunneling stage of channel flow models, although deformation timing is distinct in the different models (e.g., Fig. 2B; Beaumont et al., 2001; Webb et al., 2011b). A further distinction concerns viscosity: channel-flow tunneling models are interpreted to require exceptionally low viscosity across the GHC relative to surrounding units, which could be achieved by melt weakening (e.g., Beaumont et al., 2001, 2004). However, analogous tectonic wedging kinematics are recognized across upper crustal portions of the Canadian Cordillera (e.g., Jones, 1982; Price, 1986), where no strong viscosity contrast between units exists. Therefore, while this class of models allows large viscosity contrasts, the identification of the same bounding kinematics in largely homogeneous upper crustal rocks indicates that such viscosity contrasts are not a necessary condition for the overall kinematic evolution.

The palinspastic reconstruction indicates that the leading edge of the GHC may remain buried until ca. 5 Ma, which is later than all prior models (see review by Yin, 2006). Existing work focusing on the detrital record preserved in the Himalayan foreland rocks suggests initial GHC exhumation times ranging from ca. 40 to ca. 11 Ma (e.g., Najman et al., 2000; Yin, 2006). However, a significant challenge for interpretation of the detrital record is the close correspondence of THS and GHC provenance signals (e.g., Myrow et al., 2003; Ravikant et al., 2011). The ~5-km-thick Haimanta Group units of the THS and the GHC have the same sedimentary protoliths, Cambrian–Ordovician granitoid intrusives, and volumetrically minor leucogranite bodies (e.g., Miller et al., 2001; Webb et al., 2011a). Therefore, Nd and Sr signals used to infer ca. 40–17 Ma GHC exposure cannot distinguish THS and GHC sources (cf. France-Lanord et al., 1993; Najman et al., 2000). Other proposed GHC signals, e.g., 37–28 Ma detrital monazite, 50–20 Ma detrital mica, almandine garnet, and staurolite in the 18–11 Ma Dharamsala Formation (White et al., 2001, 2002), are well documented in the THS (Chambers et al., 2009; Webb et al., 2011a). However, the high-grade metamorphic minerals kyanite and sillimanite can be used to discriminate sedimentary products of these units, because both are abundant in the GHC and almost completely absent in the THS (e.g., Vannay and Grasemann, 1998). In the central and western Himalayan foreland, kyanite and sillimanite first appear ca. 11 Ma (DeCelles et al., 1998; White et al., 2002). This age is significantly older than the ca. 5 Ma exposure predicted by the palinspastic reconstruction. Three possibilities maintain viability of the palinspastic reconstruction. (1) Kyanite and sillimanite may be sourced from ultrahigh pressure (UHP) ter-

ranes exposed in the northern Himalaya (Yin, 2006). However, only two such terranes are known, at Kaghan Valley in Pakistan and at Tso Morari in Ladakh (e.g., Guillot et al., 2007). These each have limited exposure across only ~3000 km^2. The structural geometry at Kaghan is not well understood (Treloar et al., 2003), but the Tso Morari UHP rocks occupy the core of a regional dome, and thus are unlikely to have had more extensive exposure in the past (e.g., Steck et al., 1998; Epard and Steck, 2008). (2) Along-strike structural variation may allow earlier GHC exposure along adjacent sections. (3) GHC exposure ca. 11 Ma may have occurred along northern gneiss domes extending along the arc, such as Leo Pargil, Gurla Mandhata, and Ama Drime. Apatite fission track ages along the southern GHC exposure between the main strands of the Main Central thrust and South Tibet detachment are almost exclusively younger than 5 Ma (see reviews by Yin, 2006; Thiede et al., 2009). In contrast, ages from upper structural levels of the Leo Pargil GHC are 8–10 Ma (Thiede et al., 2006). This raises the intriguing possibility that the GHC is first exposed not along its southern front, but rather by east-west extension across the hinterland.

Ongoing Mountain Building

The restoration indicates that the dominant mode of fold-thrust belt growth since ca. 14 Ma is underplating of Lesser Himalayan Sequence slices. The first slice is a thin (~1 km thick) slice of Indian crustal basement (Baragaon granitic gneisses). The next accreted horses are the Berinag and Tons thrust hanging walls, and as these are translated, the main sole thrust cuts downsection, slicing off numerous basement slices (the Munsiari Group). For the past ~3–5 m.y., deformation appears to have been dominated by a paired duplex development; i.e., an anticlinal stack of crystalline basement slices developed synchronously with a hinterland dipping duplex of Deoban and Damtha sedimentary layers. Frontal accretion of foreland basin rocks occurs, but almost all of this material is eroded away.

This work has significant implications for the debate over out-of-sequence and underplating models for ongoing orogenesis. Most regional studies interpret Kullu window formation over the past ~10–15 m.y. to be a result of out-of-sequence faulting along the Munsiari thrust (e.g., Thiede et al., 2004, 2005, 2009; Vannay et al., 2004). The restoration includes as much as 8 km of out-of-sequence slip along the Munsiari thrust, but it shows that the Kullu window could mainly result from duplexing, in basic agreement with the underplating model (Fig. 3; Robinson et al., 2003; Bollinger et al., 2004, 2006). A critical interpretative distinction is the treatment of the Munsiari thrust hanging wall: in out-of-sequence models this is shown as a single block south of the Main Central thrust, whereas in the preliminary reconstruction the Chaura thrust splits this into two thrust sheets with distinct late Cenozoic movement histories.

The overall paired duplex development modeled for the past ~3–5 m.y. has many similarities to the analog modeling of Konstantinovskaia and Malavieille (2005, 2011) (e.g., see fig. 2C of Malavieille, 2010). Prior balancing efforts have recognized two duplexes (McQuarrie et al., 2008; Yin et al., 2010), but only the analog modeling has previously indicated the possibility of synchronous duplex development. This kinematic evolution implies that strength heterogeneities and erosion may control the deformation style since the Miocene, as in the analog models. Obvious candidates for both parameters are present, i.e., the intrabasement décollement and basement-cover décollement represent strength heterogeneities, and the Sutlej River follows the line of section above the antiformal stack, providing localized high stream power. The general position of ongoing antiformal stack development corresponds with the zone of rapid uplift documented through low-temperature thermochronology across northwestern India (cf. Thiede et al., 2009).

Parallel cross sections across the Himachal Himalaya would display significant along-strike variability in the history of mountain building over the past ~10 m.y. Along the line of section the Sutlej River localizes enhanced erosion, warping the paths of major structures (e.g., Oberlander, 1985; Thiede et al., 2004; Vannay et al., 2004; Montgomery and Stolar, 2006). In addition, the Kangra recess along the front of the Himalaya to the northwest of Shimla preserves a distinct set of structures and rocks (Fig. 4); here the slip along the Bilaspur thrust is diminished or is transferred to faults farther to the north, such that a large portion of the foreland fold-thrust belt is preserved. The Tons thrust and its hanging wall are entirely eroded away. Exposures of the Lesser Himalayan Sequence rocks thin to <5 km; in a few locations, THS rocks are thrust directly over Siwalik foreland sedimentary rocks. A similar structural pattern could be created from forward modeling of the ca. 5.4 Ma section (Plate 1E) with slip focused mainly above the Deoban-Damtha succession and the Himalayan foreland rocks. Alternatively, this pattern may result from along-strike thinning of the Deoban and Damtha rocks (Prasad et al., 2011).

Comparison of New Work to Other Balanced Palinspastic Reconstructions Across the Himalaya

There are three other recent balanced palinspastic reconstructions of Cenozoic Himalayan shortening: Long et al. (2012) restored deformation across western Bhutan, Robinson and McQuarrie (2012) provided a restoration across western Nepal, and Tobgay et al. (2012) included a restoration across eastern Bhutan. In contrast to my work, all of these reconstructions show frontal accretion as the dominant process of Himalayan mountain building since the emplacement of the Main Central thrust sheet. This process does not explain the development of the zone of rapid uplift documented across the central band of the Himalaya (e.g., Seeber and Gornitz, 1983); therefore, Long et al. (2012) proposed out-of-sequence faulting across this zone.

A central result of all three recent reconstructions is that the Himalaya has developed with dramatic changes in shortening rate since the Early and Middle Miocene. Early stages feature rapid shortening rates of as much as ~4–7 cm/yr. At the upper limit, these rates exceed the India-Asia convergence rate determined from plate circuit reconstructions during the relevant periods (i.e., during the Early and/or Middle Miocene) (cf. van Hinsbergen et al., 2011b). Late stages (from Middle Miocene to just prior to the Holocene) have slow shortening rates, as slow as 3–4 mm/yr, far slower than known Holocene and GPS geodetic slip rates of ~2 cm/yr (e.g., Lave and Avouac, 2000; Jade et al., 2004). These results contrast significantly with the interpretation presented herein, i.e., that slip rates in the Early and Middle Miocene were only slightly faster than Holocene and GPS rates, and decreased monotonically to the current rates.

This difference between my study and the existing reconstructions occurs because progressive and ongoing accretion of material at multiple crustal depths simultaneously is featured herein, whereas the other studies show dominant forward propagation of thrusting. Therefore in the other studies, material is added to the orogenic wedge exclusively at the front. Over the past few million years, these studies show almost no accretion of material other than Sub-Himalayan foreland rocks. Large volumes of the deep orogenic wedge immediately above the sole thrust are filled by thrust sheets accreted at different times in the different modeling approaches. Herein I show Pliocene to Holocene accretion to fill this space, whereas the other studies fill this space with Miocene thrust sheets. Because the other studies must therefore create the bulk of the range in the Miocene, it is not surprising that the Early and Middle

Miocene slip rates are relatively high and the subsequent rates relatively low. The relative plausibility of the two different approaches may be judged by consistency to known constraints. For example, the inability of the other studies to account for acceleration from ~3–10 mm/yr Pliocene–Pleistocene slip rates to ~20 mm/yr Holocene slip rates suggests that this study may better describe the overall accretion mode.

Western Himalayan Shortening Budget and Implications for the Greater India Basin Hypothesis

Total minimum shortening across the western Himalaya, from the suture to the undeformed foreland, can be estimated by adding the new result to prior determinations of shortening from the South Tibet detachment to the suture zone. Specifically, the new result (~518 km total shortening), estimated THS shortening (80–100 km; Searle, 1986; Steck et al., 1993; Corfield and Searle 2000), and an estimate of shortening associated with the exhumation of GHC-correlative UHP rocks at Tso Morari (~115–165 km; cf. Guillot et al., 2007) are summed, and the newly determined ~11 km of THS shortening are subtracted (because this shortening duplicates the THS shortening assessed previously; i.e., the same shortening cannot be counted twice). The resulting total shortening across the western Himalaya is ~703–773 km. This is far less than the ~1350 km of shortening predicted by plate circuit reconstructions (van Hinsbergen et al., 2011a). Was the missing shortening not recorded, perhaps supporting the Greater India Basin hypothesis, or is it poorly assessed? Here, three considerations of the missing shortening are discussed, followed by an assessment of implications for the hypothesis.

First, total shortening over the past ~14 m.y. is well preserved. For this time interval, shortening rates across the balanced palinspastic reconstruction, which are supported by thermochronological data, can be matched with a ~23 mm/yr shortening rate. This is approximately consistent with the ~19 mm/yr rate suggested by GPS studies and convergence rates deduced by analyzing (1) foreland basin propagation and overthrusting rates (e.g., Avouac, 2007) and (2) plate circuit reconstructions (e.g., Molnar and Stock, 2009). The reconstruction shows ~319 km of shortening during this period.

Second, a large portion of Himalayan shortening deformation is probably eroded away. For example, along the line of section A–A′ almost no material added to the orogen via frontal accretion before the Pliocene is preserved today (a possible exception is THS material in the far northeast) (Plate 1). This makes little difference in assessing total shortening for the past ~14 m.y., because ongoing contraction during this period was accommodated by frontal accretion of foreland basin sedimentary layers and by underplating of pre-Cenozoic rocks. The underplated rocks are largely preserved. However, if frontal accretion dominated mountain-building processes for some periods of Himalayan development, then the corresponding shortening record could have been entirely removed by erosion.

Third, there may be preserved shortening that remains unmeasured. A likely candidate is the southern THS. Existing balanced cross sections across the THS span from the Indus-Yarlung suture to the main strand of the South Tibet detachment (highlighted in Fig. 1). Shortening estimates are 80–112 km in the western and central Himalaya (Searle, 1986; Searle et al., 1997; Steck et al., 1993; Corfield and Searle, 2000; Murphy and Yin, 2003), and Ratschbacher et al. (1994) reported 258 km in the eastern Himalaya. Percent shortening is consistent at ~50%–60% (see compilation by Long et al., 2011a); therefore, the eastern total shortening may be largest because the greatest width of measured THS is preserved there. Deformed upper and/or middle crustal THS exposures locally appear much farther south than these THS balancing efforts, e.g., in Kashmir, Chamba, in the cores of southern Main Central thrust klippes in Nepal, and in South Tibet detachment klippes in Bhutan (Figs. 1 and 4) (e.g., Gansser, 1983; Gehrels et al., 2003; DiPietro and Pogue, 2004). Structural settings of some southern THS exposures are debated, but various workers have argued that some or all are contiguous with the THS to the north (e.g., Thakur and Rawat, 1992; Frank et al., 1995; Fuchs and Linner, 1995; Grujic et al., 2002; Yin, 2006; Webb et al., 2007, 2011a, 2011b; Kellett et al., 2009). The southern exposures increase the length of THS sections such that if consistent percent shortening from north to south is assumed, then minimum preserved THS shortening could exceed 500 km in the eastern Himalaya, and 300–400 km in the western Himalaya.

This third consideration suggests that the total shortening preserved across the western Himalaya ranges from ~900 to 1100 km. Because these estimates primarily result from minimum shortening estimates, they are likely directly comparable to the ~1350 km of shortening predicted by the plate circuit reconstruction (van Hinsbergen et al., 2011a). Therefore, the need for a Greater India Basin hypothesis may not exist across the western Himalaya. This hypothesis also faces another significant hurdle, i.e., the continuity of Paleozoic strata from the suture zone to the foreland. In the westernmost portions of the orogen, such strata form the hanging wall and footwall of the Main Central thrust and do not appear to contain a significant metamorphic zone that might hide a cryptic suture within these correlative rocks (Fig. 1) (Pogue et al., 1999; DiPietro and Pogue, 2004).

CONCLUSIONS

A balanced palinspastic reconstruction across the Himachal Himalaya of northwestern India reveals ~518 km (72%) shortening in the Cenozoic. This reconstruction confirms geometric viability of GHC emplacement via tectonic wedging. Furthermore, it suggests that GHC exposure along the main outcrop belt between the South Tibet detachment and Main Central thrust occurred ca. 5 Ma. Initial GHC exposure ca. 11 Ma probably occurred in the hinterland within east-west extensional core complexes. Preserved records of ongoing mountain building since the Middle Miocene are dominated by ~300 km of shortening accomplished by underplating. Deformation during the past ~3–5 m.y. features synchronous development of a leading imbricate fan, an upper crustal duplex, and a middle crustal antiformal stack. Total assessed minimum shortening across the western Himalaya is ~703–773 km, as calculated by summing our results, prior balancing across the northern THS, and basic assessment of exhumation of ultrahigh pressure rocks along the suture zone. However, large portions of the southern THS remain unmeasured, such that total preserved shortening across the western Himalaya probably ranges from minimums of ~900–1100 km. As minimums, these estimates may be directly comparable to estimates of ~1350 km derived from plate circuit reconstructions and assessment of postcollisional Asian plate shortening (van Hinsbergen et al., 2011a). The rough correspondence of geologic and plate circuit shortening estimates obviates the need for the Greater India Basin hypothesis.

ACKNOWLEDGMENTS

This work was improved significantly by thoughtful reviews by an anonymous reviewer, Joseph DiPietro, Peter DeCelles, Michael Murphy, associate editor Colin Shaw, and editor Dennis Harry. Midland Valley Exploration Ltd. staff provided able and ready assistance with Move software (http://www.mve.com/software/move). Lothar Ratschbacher and colleagues graciously hosted me at the University of Freiberg during preparation of the reconstruction. Conversations with Julien Célérier, Dennis Donaldson, Dian He, Frederic Herman, A.K. Jain, Kyle Larson, Aaron Martin, Ryan McKenzie, Mike Murphy, Birendra Singh, William Thomas, An Yin, and Hongjiao Yu greatly improved this work. This research was supported by a start-up fund from Louisiana State University and Louisiana Board of Regents grant LEQSF(2012-15)-RD-A-12.

REFERENCES CITED

Ahmad, T., Harris, N., Bickle, M., Chapman, H., Bunbury, J., and Prince, C., 2000, Isotopic constraints on the structural relationships between the lesser Himalayan series and the high Himalayan crystalline series, Garhwal Himalaya: Geological Society of America Bulletin, v. 112, p. 467–477, doi:10.1130/0016-7606(2000)112<467:ICOTSR>2.0.CO;2.

Avouac, J.P., 2003, Mountain building, erosion, and the seismic cycle in the Nepal Himalaya, *in* Dmowska, R., ed., Advances in Geophysics Volume 46: San Diego, Elsevier, p. 1–80.

Avouac, J.P., 2007, Mountain building: From earthquakes to geological deformation, *in* Schubert, G., ed., Dynamic processes in extensional and compressional settings: Treatise on Geophysics Volume 6: Cambridge, Elsevier, p. 377–439.

Beaumont, C., Jamieson, R.A., Nguyen, M.H., and Lee, B., 2001, Himalayan tectonics explained by extrusion of a low-viscosity crustal channel coupled to focused surface denudation: Nature, v. 414, p. 738–742, doi:10.1038/414738a.

Beaumont, C., Jamieson, R.A., Nguyen, M.H., and Medvedev, S., 2004, Crustal channel flows: 1. Numerical models with applications to the tectonics of the Himalayan-Tibetan orogen: Journal of Geophysical Research, v. 109, B06406, doi:10.1029/2003JB002809.

Blythe, A.E., Burbank, D.W., Carter, A., Schmidt, K., and Putkonen, J., 2007, Plio-Quaternary exhumation history of the central Nepalese Himalaya: 1. Apatite and zircon fission-track and apatite [U-Th]/He analyses: Tectonics, v. 26, doi:10.1029/2006TC001990.

Bollinger, L., Avouac, J.P., Beyssac, O., Catlos, E.J., Harrison, T.M., Grove, M., Goffé, B., and Sapkota, S., 2004, Thermal structure and exhumation history of the Lesser Himalaya in central Nepal: Tectonics, v. 23, TC5015, doi:10.1029/2003TC001564.

Bollinger, L., Henry, P., and Avouac, J.P., 2006, Mountain building in the Nepal Himalaya: Thermal and kinematic model: Earth and Planetary Science Letters, v. 244, p. 58–71, doi:10.1016/j.epsl.2006.01.045.

Bookhagen, B., and Burbank, D.W., 2006, Topography, relief, and TRMM-derived rainfall variations along the Himalaya: Geophysical Research Letters, v. 33, doi:10.1029/2006GL026037.

Burbank, D.W., Blythe, A.E., Putkonen, J., Pratt-Sitaula, B., Gabet, E., Oskin, M., Barros, A., and Ojha, T.P., 2003, Decoupling of erosion and precipitation in the Himalayas: Nature, v. 426, p. 652–655, doi:10.1038/nature02187.

Burchfiel, B.C., and Royden, L.H., 1985, North-south extension within the convergent Himalayan region: Geology, v. 13, p. 679–682, doi:10.1130/0091-7613(1985)13<679:NEWTCH>2.0.CO;2.

Burchfiel, B.C., Zhiliang, C., Hodges, K.V., Yuping, L., Royden, L.H., Changrong, D., and Jiene, X., 1992, The South Tibetan Detachment System, Himalayan orogen: Extension contemporaneous with and parallel to shortening in a collisional mountain belt: Geological Society of America Special Paper 269, 41 p., doi:10.1130/SPE269-p1.

Burg, J.P., Brunel, M., Gapais, D., Chen, G.M., and Liu, G.H., 1984, Deformation of leucogranites of the crystalline Main Central Sheet in southern Tibet (China): Journal of Structural Geology, v. 6, p. 535–542, doi:10.1016/0191-8141(84)90063-4.

Caddick, M.J., Bickle, M.J., Harris, N.B.W., Holland, T.J.B., Horstwood, M.S.A., Parrish, R.R., and Ahmad, T., 2007, Burial and exhumation history of a Lesser Himalayan schist: Recording the formation of an inverted metamorphic sequence in NW India: Earth and Planetary Science Letters, v. 264, p. 375–390, doi:10.1016/j.epsl.2007.09.011.

Cande, S.C., Patriat, P., and Dyment, J., 2010, Motion between the Indian, Antarctica and African plates in the early Cenozoic: Geophysical Journal International, v. 183, p. 127–149, doi:10.1111/j.1365-246X.2010.04737.x.

Célérier, J., Harrison, T.M., Webb, A.A.G., and Yin, A., 2009a, The Kumaun and Garwhal Lesser Himalaya, India; Part 1, Structure and stratigraphy: Geological Society of America Bulletin, v. 121, p. 1262–1280, doi:10.1130/B26344.1.

Célérier, J., Harrison, T.M., Beyssac, O., Herman, F., Dunlap, W.J., and Webb, A.A.G., 2009b, The Kumaun and Garwhal Lesser Himalaya, India; Part 2, Thermal and deformation histories: Geological Society of America Bulletin, v. 121, p. 1281–1297, doi:10.1130/B26343.1.

Chambers, J.A., Argles, T.W., Horstwood, M.S.A., Harris, N.B.W., Parrish, R.R., and Ahmad, T., 2008, Tectonic implications of Palaeoproterozoic anatexis and Late Miocene metamorphism in the Lesser Himalayan Sequence, Sutlej Valley, NW India: Geological Society of London Journal, v. 165, p. 725–737, doi:10.1144/0016-76492007/090.

Chambers, J., Caddick, M., Argles, T., Horstwood, M., Sherlock, S., Harris, N., Parrish, R., and Ahmad, T., 2009, Empirical constraints on extrusion mechanisms from the upper margin of an exhumed high-grade orogenic core, Sutlej valley, NW India: Tectonophysics, v. 477, p. 77–92, doi:10.1016/j.tecto.2008.10.013.

Clift, P.D., Hodges, K., Heslop, D., Hannigan, R., Hoang, L.V., and Calves, G., 2008, Correlation of Himalayan exhumation rates and Asian monsoon intensity: Nature Geoscience, v. 1, p. 875–880, doi:10.1038/ngeo351.

Cook, B.S., and Thomas, W.A., 2010, Ductile duplexes as potential natural gas plays: An example from the Appalachian thrust belt in Georgia, USA, *in* Goffey, G.P., et al., eds., Hydrocarbons in contractional belts: Geological Society London Special Publication 348, 57–70, doi:10.1144/SP348.4.

Copley, A., Avouac, J.P., and Royer, J.Y., 2010, The India-Asia collision and the Cenozoic slowdown of the Indian plate: Implications for the forces driving plate motions: Journal of Geophysical Research, v. 115, B03410, doi:10.1029/2009JB006634.

Corfield, R.I., and Searle, M.P., 2000, Crustal shortening estimates across the north Indian continental margin, Ladakh, NW India, *in* Khan, M.A., et al., eds., Tectonics of the Nanga Parbat syntaxis and the Western Himalaya: Geological Society of London Special Publication 170, p. 395–410, doi:10.1144/GSL.SP.2000.170.01.21.

Corrie, S.L., and Kohn, M.J., 2011, Metamorphic history of the central Himalaya, Annapurna region, Nepal, and implications for tectonic models: Geological Society of America Bulletin, v. 123, p. 1863–1879, doi:10.1130/B30376.1.

Dahlen, F.A., 1990, Critical taper model of fold-and-thrust belts and accretionary wedges: Annual Review of Earth and Planetary Sciences, v. 18, p. 55-99.

Das, B.K., and Rastogi, R.G., 1988, Petrology of Jutogh metapelites near Chaur, Himachal Himalaya, India: Geological Society of India Journal, v. 31, p. 251–266.

Davis, D., Suppe, J., and Dahlen, F.A., 1983, Mechanics of fold-and-thrust belts and accretionary wedges: Journal of Geophysical Research, v. 88, no. B2, p. 1153–1178, doi:10.1029/JB088iB02p01153.

DeCelles, P.G., Gehrels, G.E., Quade, J., Ojha, T.P., Kapp, P.A., and Upreti, B.N., 1998, Neogene foreland basin deposits, erosional unroofing, and the kinematic history of the Himalayan fold-thrust belt, western Nepal: Geological Society of America Bulletin, v. 110, p. 2–21.

DeCelles, P.G., Robinson, D.M., Quade, J., Ojha, T.P., Garzione, C.N., Copeland, P., and Upreti, B.N., 2001, Stratigraphy, structure, and tectonic evolution of the Himalayan fold–thrust belt in western Nepal: Tectonics, v. 20, p. 487–509, doi:10.1029/2000TC001226.

DeCelles, P.G., Kapp, P., Quade, J., and Gehrels, G.E., 2011, Oligocene–Miocene Kailas Basin, southwestern Tibet: Record of postcollisional upper-plate extension in the Indus-Yarlung suture zone: Geological Society of America Bulletin, v. 123, p. 1337–1362, doi:10.1130/B30258.1.

Dewey, J.F., Cande, S., and Pitman, W.C., 1989, Tectonic evolution of the India/Eurasia collision zone: Eclogae Geologicae Helvetiae, v. 82, p. 717–734.

DiPietro, J.A., and Pogue, K.R., 2004, Tectonostratigraphic subdivisions of the Himalaya: A view from the west: Tectonics, v. 23, TC5001, doi:10.1029/2003TC001554.

Dupont-Nivet, G., Lippert, P., van Hinsbergen, D.J.J., Meijers, M.J.M., and Kapp, P., 2010, Paleolatitude and age of the Indo-Asia collision: Paleomagnetic constraints: Geophysical Journal International, v. 182, p. 1189–1198, doi:10.1111/j.1365-246X.2010.04697.x.

Epard, J.L., and Steck, A., 2008, Structural development of the Tso Morari ultra-high pressure nappe of the Ladakh Himalaya: Tectonophysics, v. 451, p. 242–264, doi:10.1016/j.tecto.2007.11.050.

France-Lanord, C., Derry, L., and Michard, A., 1993, Evolution of the Himalaya since Miocene time: Isotopic and sedimentological evidence from the Bengal fan, *in* Treloar, P.J., and Searle, M.P., eds., Himalayan tectonics: Geological Society of London Special Publication 74, p. 603–621, doi:10.1144/GSL.SP.1993.074.01.40.

Frank, W., Grasemann, B., Guntli, P., and Miller, C., 1995, Geological map of the Kishtwar–Chamba–Kulu region (NW Himalayas, India): Jahrbuch der Geologischen Bundesanstalt, v. 138, p. 208–299.

Fuchs, G., and Linner, M., 1995, Geological traverse across the western Himalaya; A contribution to the geology of eastern Ladakh, Lahul, and Chamba: Jahrbuch der Geologischen Bundesanstalt Wien, v. 138, no. 4, p. 655–685.

Gansser, A., 1964, The geology of the Himalayas: New York, Wiley Interscience, 289 p.

Gansser, A., 1983, Geology of the Bhutan Himalaya: Boston, Birkhäuser Verlag, 180 p.

Gehrels, G.E., DeCelles, P.G., Martin, A., Ojha, T.P., Pinhassi, G., and Upreti, B.N., 2003, Initiation of the Himalayan orogen as an early Paleozoic thin-skinned thrust belt: GSA Today, v. 13, no. 9, p. 4–9, doi:10.1130/1052-5173(2003)13<4:IOTHOA>2.0.CO;2.

Gregory, C., 2004, Microstructural analysis of the Main Central thrust, North West Himalaya (India) [thesis]: Canberra, Australia National University, 79 p.

Grujic, D., Casey, M., Davidson, C., Hollister, L.S., Kundig, R., Pavlis, T., and Schmid, S., 1996, Ductile extrusion of the Higher Himalayan Crystalline in Bhutan: Evidence form quartz microfabrics: Tectonophysics, v. 260, p. 21–43, doi:10.1016/0040-1951(96)00074-1.

Grujic, D., Hollister, L.S., and Parrish, R.R., 2002, Himalayan metamorphic sequence as an orogenic channel: Insight from Bhutan: Earth and Planetary Science Letters, v. 198, p. 177–191, doi:10.1016/S0012-821X(02)00482-X.

Guillot, S., Replumaz, A., Hattori, K.H., and Strzerzynski, P., 2007, Initial geometry of western Himalaya and ultrahigh-pressure metamorphic evolution: Journal of Asian Earth Sciences, v. 30, p. 557–564, doi:10.1016/j.jseaes.2007.01.004.

Harrison, T.M., Ryerson, F.J., Le Fort, P., Yin, A., Lovera, O.M., and Catlos, E.J., 1997, A Late Miocene–Pliocene origin for the Central Himalayan inverted metamorphism: Earth and Planetary Science Letters, v. 146, p. 1–7, doi:10.1016/S0012-821X(96)00215-4.

Harrison, T.M., Yin, A., Grove, M., Lovera, O.M., Ryerson, F.J., and Zhou, X.H., 2000, The Zedong window: A record of superposed Tertiary convergence in southeastern Tibet: Journal of Geophysical Research, v. 105, p. 19,211–19,230, doi:10.1029/2000JB900078.

Heim, A., and Gansser, A., 1939, Central Himalaya geological observations of the Swiss Expedition 1936: Zurich, Gebrüder Fretz, 246 p.

Herman, F., Copeland, P., Avouac, J.P., Bollinger, L., Maheo, G., Le Fort, P., Rai, S., Foster, D., Pecher, A., Stuwe, K., and Henry, P., 2010, Exhumation, crustal deformation, and thermal structure of the Nepal Himalaya derived from the inversion of thermochronological and thermobarometric data and modeling of the topography: Journal of Geophysical Research, v. 115, no. B6, doi:10.1029/2008JB006126.

Hodges, K.V., 2000, Tectonics of the Himalaya and southern Tibet from two perspectives: Geological Society of America Bulletin, v. 112, p. 324–350, doi:10.1130/0016-7606(2000)112<324:TOTHAS>2.0.CO;2.

Hodges, K.V., Parrish, R.R., Housh, T.B., Lux, D.R., Burchfiel, B.C., Royden, L.H., and Chen, Z., 1992, Simultaneous Miocene extension and shortening in the Himalayan orogen: Science, v. 258, no. 5087, p. 1466–1470, doi:10.1126/science.258.5087.1466.

Hodges, K.V., Parrish, R.R., and Searle, M.P., 1996, Tectonic evolution of the central Annapurna Range, Nepalese Himalayas: Tectonics, v. 15, p. 1264–1291, doi:10.1029/96TC01791.

Hodges, K.V., Hurtado, J.M., and Whipple, K.X., 2001, Southward extrusion of Tibetan crust and its effect on

Himalayan tectonics: Tectonics, v. 20, p. 799–809, doi: 10.1029/2001TC001281.

Huntington, K., Blythe, A.E., and Hodges, K.V., 2006, Climate change and Late Pliocene acceleration of erosion in the Himalaya: Earth and Planetary Science Letters, v. 252, p. 107–118, doi:10.1016/j.epsl.2006.09.031.

Jade, S., Bhatt, B.C., Yang, Z., Bendick, R., Gaur, V.K., Molnar, P., Anand, M.B., and Kumar, D., 2004, GPS measurements from the Ladakh Himalaya, India; preliminary tests of plate-like or continuous deformation in Tibet: Geological Society of America Bulletin, v. 116, p. 1385–1391, doi:10.1130/B25357.1.

Jain, A.K., and Manickavasagam, R.M., 1993, Inverted metamorphism in the intracontinental ductile shear zone during Himalayan collision tectonics: Geology, v. 21, p. 407–410, doi:10.1130/0091-7613(1993)021<0407:IMITID>2.3.CO;2.

Jain, A.K., Manickavasagam, R.M., and Singh, S., 1999, Collision tectonics in the NW Himalaya: Deformation, metamorphism, emplacement of leucogranite along Beas-Parbati Valleys, Himachal Pradesh: Gondwana Research Group Memoir 6, p. 3–37.

Jain, A.K., Kumar, D., Singh, S., Kumar, A., and Lal, N., 2000, Timing, quantification and tectonic modelling of Pliocene–Quaternary movements in the NW Himalaya: Evidence from fission track dating: Earth and Planetary Science Letters, v. 179, p. 437–451, doi:10.1016/S0012-821X(00)00133-3.

Jones, P.B., 1982, Oil and gas beneath east-dipping underthrust faults in the Alberta Foothills, *in* Powers, R.B., ed., Geological studies of the Cordilleran thrust belt: Denver, Colorado, Rocky Mountain Association of Petroleum Geologists, p. 61–74.

Kellett, D.A., and Grujic, D., 2012, New insight into the South Tibetan detachment system: Not a single progressive deformation: Tectonics, v. 31, TC2007, doi: 10.1029/2011TC002957.

Kellett, D.A., Grujic, D., and Erdmann, S., 2009, Miocene structural reorganization of the South Tibetan detachment, eastern Himalaya: Implications for continental collision: Lithosphere, v. 1, p. 259–281, doi:10.1130/L56.1.

Kohn, M.J., 2008, P–T–t data from central Nepal support critical taper and repudiate large-scale channel flow of the Greater Himalayan Sequence: Geological Society of America Bulletin, v. 120, p. 259–273, doi:10.1130/B26252.1.

Kohn, M.J., Wieland, M.S., Parkinson, C.D., and Upreti, B.N., 2004, Miocene faulting at plate tectonic velocity in the Himalaya of central Nepal: Earth and Planetary Science Letters, v. 228, p. 299-310.

Konstantinovskaia, E., and Malavieille, J., 2005, Erosion and exhumation in accretionary orogens: Experimental and geological approaches: Geochemistry Geophysics Geosystems, v. 6, doi:10.1029/2004GC000794.

Konstantinovskaia, E., and Malavieille, J., 2011, Thrust wedges with décollement levels and syntectonic erosion: A view from analog models: Tectonophysics, v. 502, p. 336–350, doi:10.1016/j.tecto.2011.01.020.

Lave, J., and Avouac, J.P., 2000, Active folding of fluvial terraces across the Siwaliks Hills, Himalayas of central Nepal: Journal of Geophysical Research, v. 105, p. 5735–5770, doi:10.1029/1999JB900292.

Lave, J., and Avouac, J.P., 2001, Fluvial incision and tectonic uplift across the Himalaya of central Nepal: Journal of Geophysical Research, v. 106, p. 26561–26591, doi:10.1029/2001JB000359.

Le Fort, P., 1975, Himalayas–collided range–present knowledge of continental arc: American Journal of Science, v. A275, p. 1–44.

Leger, R.M., Webb, A.A.G., Henry, D.J., Craig, J.A., and Dubey, P., 2013, Metamorphic field gradients across the Himachal Himalaya, northwest India: Implications for the emplacement of the Himalayan crystalline core: Tectonics, doi:10.1002/tect.20020 (in press).

Long, S., McQuarrie, N., Tobgay, T., and Grujic, D., 2011a, Geometry and crustal shortening of the Himalayan fold-thrust belt, eastern and central Bhutan: Geological Society of America Bulletin, v. 123, p. 1427–1447, doi:10.1130/B30203.1.

Long, S., McQuarrie, N., Tobgay, T., and Hawthorne, J., 2011b, Quantifying internal strain and deformation temperature in the eastern Himalaya, Bhutan: Implications for the evolution of strain in thrust sheets: Journal of Structural Geology, v. 33, p. 579–608, doi:10.1016/j.jsg.2010.12.011.

Long, S., McQuarrie, N., Tobgay, T., Coutand, I., Cooper, F.J., Reiners, P.W., Wartho, J.-A., and Hodges, K.V., 2012, Variable shortening rates in the eastern Himalayan thrust belt, Bhutan: Insights from multiple thermochronologic and geochronologic data sets tied to kinematic reconstructions: Tectonics, v. 31, TC5004, doi:10.1029/2012TC003155.

Malavieille, J., 2010, Impact of erosion, sedimentation, and structural heritage on the structure and kinematics of orogenic wedges: Analog models and case studies: GSA Today, v. 20, p. 4–10, doi:10.1130/GSATG48A.1.

McKenzie, N.R., Hughes, N.C., Myrow, P.M., Xiao, S., and Sharma, M., 2011, Correlation of Precambrian Cambrian sedimentary successions across northern India and the utility of isotopic signatures of Himalayan lithotectonic zones: Earth and Planetary Science Letters, v. 312, p. 471–483, doi:10.1016/j.epsl.2011.10.027.

McQuarrie, N., Robinson, D., Long, S., Tobgay, T., Grujic, D., Gehrels, G., and Ducea, M., 2008, Preliminary stratigraphic and structural architecture of Bhutan: Implications for the along strike architecture of the Himalayan system: Earth and Planetary Science Letters, v. 272, p. 105–117, doi:10.1016/j.epsl.2008.04.030.

Miller, C., Thoni, M., Frank, W., Grasemann, B., Klotzli, U., Guntli, P., and Draganits, E., 2001, The early Palaeozoic magmatic event in the Northwest Himalaya, India: Source, tectonic setting and age of emplacement: Geological Magazine, v. 138, p. 237–251, doi:10.1017/S0016756801005283.

Molnar, P., and England, P., 1990, Late Cenozoic uplift of mountain ranges and global climate change: Chicken or egg?: Nature, v. 346, p. 29–34, doi:10.1038/346029a0.

Molnar, P., and Stock, J.M., 2009, Slowing of India's convergence with Eurasia since 20 Ma and its implications for Tibetan mantle dynamics: Tectonics, v. 28, TC3001, doi:10.1029/2008TC002271.

Molnar, P., and Tapponnier, P., 1975, Cenozoic tectonics of Asia: Effects of a continental collision: Science, v. 189, p. 419–426, doi:10.1126/science.189.4201.419.

Montgomery, D.R., and Stolar, D.B., 2006, Reconsidering Himalayan river anticlines: Geomorphology, v. 82, p. 4–15, doi:10.1016/j.geomorph.2005.08.021.

Murphy, M.A., 2007, Isotopic characteristics of the Gurla Mandhata metamorphic core complex: Implications for the architecture of the Himalayan orogen: Geology, v. 35, p. 983–986, doi:10.1130/G23774A.1.

Murphy, M.A., and Copeland, P., 2005, Transtensional deformation in the central Himalaya and its role in accommodating growth of the Himalayan orogen: Tectonics, v. 24, TC4012, doi:10.1029/2004TC001659.

Murphy, M.A., and Yin, A., 2003, Structural evolution and sequence of thrusting in the Tethyan fold-thrust belt and Indus-Yalu suture zone, southwest Tibet: Geological Society of America Bulletin, v. 115, p. 21–34, doi:10.1130/0016-7606(2003)115<0021:SEASOT>2.0.CO;2.

Murphy, M.A., Saylor, J.E., and Ding, L., 2009, Late Miocene topographic inversion in southwest Tibet based on integrated paleoelevation reconstructions and structural history: Earth and Planetary Science Letters, v. 282, p. 1–9, doi:10.1016/j.epsl.2009.01.006.

Myrow, P.M., Hughes, N.C., Paulsen, T.S., Willlams, I.S., Parcha, S.K., Thompson, K.R., Bowring, S.A., Peng, S.C., and Ahluwalia, A.D., 2003, Integrated tectonostratigraphic analysis of the Himalaya and implications for its tectonic reconstruction: Earth and Planetary Science Letters, v. 212, p. 433–441, doi:10.1016/S0012-821X(03)00280-2.

Najman, Y., Bickle, M., and Chapman, H., 2000, Early Himalayan exhumation: Isotopic constraints from the Indian foreland basin: Terra Nova, v. 12, p. 28–34, doi: 10.1046/j.1365-3121.2000.00268.x.

Nelson, K.D., and 27 others, 1996, Partially molten middle crust beneath southern Tibet: Synthesis of Project INDEPTH results: Science, v. 274, p. 1684–1688, doi: 10.1126/science.274.5293.1684.

Oberlander, T.M., 1985, Origin of drainage transverse to structures in orogens, *in* Morisawa, M., and Hack, J.T., eds., Tectonic geomorphology: Binghamton Symposia in Geomorphology, International Series 15: Boston, Massachusetts, Allen and Unwin, p. 155–182.

Patriat, P., and Achache, J., 1984, India-Eurasia collision chronology has implications for crustal shortening and driving mechanism of plates: Nature, v. 311, p. 615–621, doi:10.1038/311615a0.

Pogue, K.R., Hylland, M.D., Yeats, R.S., Khattak, W.U., and Hussain, A., 1999, Stratigraphic and structural framework of Himalayan foothills, northern Pakistan, *in* Macfarlane, A., et al., eds., Himalaya and Tibet: Mountain roots to mountain tops: Geological Society of America Special Paper 328, p. 257–274, doi:10.1130/0-8137-2328-0.257.

Powers, P.M., Lillie, R.J., and Yeats, R.S., 1998, Structure and shortening of the Kangra and Dehra Dun reentrants, Sub-Himalaya, India: Geological Society of America Bulletin, v. 110, p. 1010–1027, doi:10.1130/0016-7606(1998)110<1010:SASOTK>2.3.CO;2.

Prasad, B.R., Klemperer, S.L., Rao, V.V., Tewari, H.C., and Khare, P., 2011, Crustal structure beneath the Sub-Himalayan fold-thrust belt, Kangra recess, northwest India, from seismic reflection profiling: Implications for late Paleoproterozoic orogenesis and modern earthquake hazard: Earth and Planetary Science Letters, v. 308, p. 218–228, doi:10.1016/j.epsl.2011.05.052.

Price, R.A., 1986, The southeastern Canadian Cordillera: Thrust faulting, tectonic wedging, and delamination of the lithosphere: Journal of Structural Geology, v. 8, p. 239–254, doi:10.1016/0191-8141(86)90046-5.

Price, R.A., 1988, The mechanical paradox of large overthrusts: Geological Society of America Bulletin, v. 100, p. 1898–1908, doi:10.1130/0016-7606(1988)100<1898:TMPOLO>2.3.CO;2.

Ratschbacher, L., Frisch, W., Liu, G., and Chen, C., 1994, Distributed deformation in southern and western Tibet during and after the India-Asia collision: Journal of Geophysical Research, v. 99, p. 19917–19945, doi: 10.1029/94JB00932.

Ravikant, V., Wu, F.-Y., and Ji, W.-Q., 2011, U-Pb age and Hf isotopic constraints of detrital zircons from the Himalayan foreland Subathu sub-basin on the Tertiary palaeogeography of the Himalaya: Earth and Planetary Science Letters, v. 304, p. 356–368, doi:10.1016/j.epsl.2011.02.009.

Richards, A., Argles, T., Harris, N., Parrish, R., Ahmad, T., Darbyshire, F., and Draganits, E., 2005, Himalayan architecture constrained by isotopic tracers from clastic sediments: Earth and Planetary Science Letters, v. 236, p. 773–796, doi:10.1016/j.epsl.2005.05.034.

Robinson, D.M., and McQuarrie, N., 2012, Pulsed deformation and variable slip rates within the central Himalayan thrust belt: Lithosphere, v. 4, p. 449–464, doi: 10.1130/L204.1.

Robinson, D.M., DeCelles, P.G., Garzione, C.N., Pearson, O.N., Harrison, T.M., Catlos, E.J., 2003, Kinematic model for the Main Central thrust in Nepal: Geology, v. 31, p. 359–362, doi:10.1130/0091-7613(2003)031<0359:KMFTMC>2.0.CO;2.

Robinson, D.M., DeCelles, P.G., and Copeland, P., 2006, Tectonic evolution of the Himalayan thrust belt in western Nepal: Implications for channel flow models: Geological Society of America Bulletin, v. 118, p. 865–885, doi:10.1130/B25911.1.

Schelling, D., and Arita, K., 1991, Thrust tectonics, crustal shortening, and the structure of the far-eastern Nepal, Himalaya: Tectonics, v. 10, p. 851–862, doi:10.1029/91TC01011.

Schlup, M., Steck, A., Carter, A., Cosca, M., Epard, J.L., and Hunziker, J., 2011, Exhumation history of the NW Indian Himalaya revealed by fission track and $^{40}Ar/^{39}Ar$ ages: Journal of Asian Earth Sciences, v. 40, p. 334–350, doi:10.1016/j.jseaes.2010.06.008.

Searle, M.P., 1986, Structural evolution and sequence of thrusting in the High Himalayan, Tibetan Tethyan and Indus suture zones of Zanskar and Ladakh, western Himalaya: Journal of Structural Geology, v. 8, p. 923–936, doi:10.1016/0191-8141(86)90037-4.

Searle, M.P., 2010, Low-angle normal faults in the compressional Himalayan orogen; evidence from the Annapurna-Dhaulagiri Himalaya, Nepal: Geosphere, v. 6, p. 296–315, doi:10.1130/GES00549.1.

Searle, M.P., Corfield, R.I., Stephenson, B., and McCarron, J., 1997, Structure of the North Indian continental margin in the Ladakh-Zanskar Himalayas: Implications for the timing of obduction of the Spontang ophiolite, India-Asia collision and deformation events in the Himalaya: Geological Magazine, v. 134, p. 297–316, doi:10.1017/S0016756897006857.

Seeber, L., and Gornitz, V., 1983, River profiles along the Himalayan arc as indicators of active tectonics: Tectonophysics, v. 92, p. 335–367, doi:10.1016/0040-1951(83)90201-9.

Singh, S., and Jain, A.K., 1996, Ductile shearing of the Proterozoic Chor Granitoid in the Lesser Himalaya and its tectonic significance: Journal of the Geological Society of India, v. 47, p. 133-138.

Srikantia, S.V., and Sharma, R.P., 1976, Geology of the Shali Belt and the adjoining areas: Memoirs of the Geological Survey of India, v. 106, p. 31–66.

Srivastava, P., and Mitra, G., 1994, Thrust geometries and deep structure of the outer and lesser Himalaya, Kumaon and Garhwal (India): Implications for evolution of the Himalayan fold-and-thrust belt: Tectonics, v. 13, p. 89–109, doi:10.1029/93TC01130.

Steck, A., Spring, L., Vannay, J.-C., Masson, H., Bucher, H., Stutz, E., Marchant, R., and Tieche, J.-C., 1993, The tectonic evolution of the Northwestern Himalaya in eastern Ladakh and Lahul, India, *in* Treloar, P.J., and Searle, M.P. eds., Himalayan tectonics: Geological Society of London Special Publication 74, pp. 265–276, doi:10.1144/GSL.SP.1993.074.01.19.

Steck, A., Epard, J.-L., Vannay, J.-C., Hunziker, J., Girard, M., Morard, A., and Robyr, M., 1998, Geological transect across the Tso Morari and Spiti areas: The nappe structures of the Tethys Himalaya: Eclogae Geologicae Helvetiae, v. 91, p. 103–121.

Thakur, V.C., 1998, Structure of the Chamba nappe and position of the main central thrust in Kashmir Himalaya: Journal of Asian Earth Sciences, v. 16, p. 269–282, doi:10.1016/S0743-9547(98)00011-7.

Thakur, V.C., and Rawat, B.S., 1992, Geologic map of Western Himalaya: Dehra Dun, India, Wadia Institute of Himalayan Geology, scale 1:1,000,000.

Thiede, R.C., Bookhagen, B., Arrowsmith, J.R., Sobel, E.R., and Strecker, M.R., 2004, Climatic control on rapid exhumation along the Southern Himalayan Front: Earth and Planetary Science Letters, v. 222, p. 791–806, doi:10.1016/j.epsl.2004.03.015.

Thiede, R.C., Arrowsmith, J.R., Bookhagen, B., McWilliams, M.O., Sobel, E.R., and Strecker, M.R., 2005, From tectonically to erosionally controlled development of the Himalayan fold-and-thrust belt: Geology, v. 33, p. 689–692, doi:10.1130/G21483.1.

Thiede, R.C., Arrowsmith, J.R., Bookhagen, B., McWilliams, M., Sobel, E.R., and Strecker, M.R., 2006, Dome formation and extension in the Tethyan Himalaya, Leo Pargil, northwest India: Geological Society of America Bulletin, v. 118, p. 635–650, doi:10.1130/B25872.1.

Thiede, R.C., Ehlers, T.A., Bookhagen, B., and Strecker, M.R., 2009, Erosional variability along the northwest Himalaya: Journal of Geophysical Research, v. 114, no. F1, doi:10.1029/2008JF001010.

Thomas, W.A., 2001, Mushwad: Ductile duplex in the Appalachian thrust belt in Alabama: American Association of Petroleum Geologists Bulletin, v. 85, p. 1847–1869.

Tobgay, T., McQuarrie, N., Long, S., Kohn, M.J., and Corrie, S.L., 2012, The age and rate of displacement along the Main Central Thrust in the western Bhutan Himalaya: Earth and Planetary Science Letters, v. 319–320, p. 146–158, doi:10.1016/j.epsl.2011.12.005.

Torsvik, T.H., Müller, R.D., Van der Voo, R., Steinberger, B., and Gaina, C., 2008, Global plate motion frames: Toward a unified model: Reviews of Geophysics, v. 46, RG3004, doi:10.1029/2007RG000227.

Treloar, P.J., O'Brien, P.J., Parrish, R.R., and Khan, M.A., 2003, Exhumation of early Tertiary, coesite-bearing eclogites from the Pakistan Himalaya: Geological Society of London Journal, v. 160, p. 367–376, doi:10.1144/0016-764902-075.

Upreti, B.N., 1999, An overview of the stratigraphy and tectonics of the Nepal Himalaya: Journal of Asian Earth Sciences, v. 17, p. 577–606, doi:10.1016/S1367-9120(99)00047-4.

Valdiya, K.S., 1980, Geology of Kumaun Lesser Himalaya: Dehra Dun, India, Wadia Institute of Himalayan Geology, 291 p.

van Hinsbergen, D.J.J., Kapp, P., Dupont-Nivet, G., Lippert, P.C., DeCelles, P.G., and Torsvik, T.H., 2011a, Restoration of Cenozoic deformation in Asia and the size of greater India: Tectonics, v. 30, TC5003, doi:10.1029/2011TC002908.

van Hinsbergen, D.J.J., Steinberger, B., Doubrovine, P.V., and Gassmöller, R., 2011b, Acceleration and deceleration of India-Asia convergence since the Cretaceous: Roles of mantle plumes and continental collision: Journal of Geophysical Research, v. 116, B06101, doi:10.1029/2010JB008051.

van Hinsbergen, D.J.J., Lippert, P.C., Dupont-Nivet, G., McQuarrie, N., Doubrovine, P.V., Spakman, W., Torsvik, T.H., 2012, Greater India Basin hypothesis and a two-stage Cenozoic collision between India and Asia: National Academy of Sciences Proceedings, doi:10.1073/pnas.1117262109.

Vannay, J.C., and Grasemann, B., 1998, Inverted metamorphism in the High Himalaya of Himachal Pradesh (NW India): Phase equilibria versus thermobarometry: Schweizerische Mineralogische und Petrographische Mitteilungen, v. 78, p. 107–132.

Vannay, J.C., and Steck, A., 1995, Tectonic evolution of the High Himalaya in Upper Lahul (NW Himalaya, India): Tectonics, v. 14, p. 253–263, doi:10.1029/94TC02455.

Vannay, J.C., Sharp, Z.D., and Grasemann, B., 1999, Himalayan inverted metamorphism constrained by oxygen isotope thermometry: Contributions to Mineralogy and Petrology, v. 137, p. 90–101, doi:10.1007/s004100050584.

Vannay, J.C., Grasemann, B., Rahn, M., Frank, W., Carter, A., Baudraz, V., and Cosca, M., 2004, Miocene to Holocene exhumation of metamorphic crustal wedges in the NW Himalaya: Evidence for tectonic extrusion coupled to fluvial erosion: Tectonics, v. 23, TC1014, doi:10.1029/2002TC001429.

Webb, A.A.G., 2007, Contractional and extensional tectonics during the India-Asia collision [Ph.D. thesis]: University of California at Los Angeles, 246 p.

Webb, A.A.G., Yin, A., Harrison, T.M., Célérier, J., and Burgess, W.P., 2007, The leading edge of the Greater Himalayan Crystallines revealed in the NW Indian Himalaya: Implications for the evolution of the Himalayan Orogen: Geology, v. 35, p. 955–958, doi:10.1130/G23931A.1.

Webb, A.A.G., Yin, A., Harrison, T.M., Célérier, J., Gehrels, G.E., Manning, C.E., and Grove, M., 2011a, Cenozoic tectonic history of the Himachal Himalaya (northwestern India) and its constraints on the formation mechanism of the Himalayan orogen: Geosphere, v. 7, p. 1013–1061, doi:10.1130/GES00627.1.

Webb, A.A.G., Schmitt, A.K., He, D., and Weigand, E.L., 2011b, Structural and geochronological evidence for the leading edge of the Greater Himalayan Crystalline complex in the central Nepal Himalaya: Earth and Planetary Science Letters, v. 304, p. 483–495, doi:10.1016/j.epsl.2011.02.024.

Webb, A.A.G., Yin, A., and Dubey, C.S., 2013, U-Pb zircon geochronology of major lithologic units in the Eastern Himalaya: Implications for the origin and assembly of Himalayan rocks: Geological Society of America Bulletin, v. 125, p. 499-522.

Whipp, D.M., Jr., Ehlers, T.A., Blythe, A.E., Huntington, K.W., Hodges, K.V., Burbank, D., 2007, Plio-Quaternary exhumation history of the central Nepalese Himalya; 2, Thermokinematic and thermochronometer age prediction model: Tectonics, v. 26, no. 3, doi:10.1029/2006TC001991.

White, L.T., and Lister, G.S., 2012, The collision of India with Asia: Journal of Geodynamics, v. 56–57, p. 7–17, doi:10.1016/j.jog.2011.06.006.

White, N.M., Parrish, R.R., Bickle, M.J., Najman, Y.M.R., Burbank, D., and Maithani, A., 2001, Metamorphism and exhumation of the NW Himalaya constrained by U-Th-Pb analyses of detrital monazite grains from early foreland basin sediments: Geological Society of London Journal, v. 158, p. 625–635, doi:10.1144/jgs.158.4.625.

White, N.M., Pringle, M., Garzanti, E., Bickle, M., Najman, Y., Chapman, H., and Friend, P., 2002, Constraints on the exhumation and erosion of the High Himalayan Slab, NW India, from foreland basin deposits: Earth and Planetary Science Letters, v. 195, p. 29–44, doi:10.1016/S0012-821X(01)00565-9.

Wiesmayr, G., and Grasemann, B., 2002, Eohimalayan fold and thrust belt: Implications for the geodynamic evolution of the NW-Himalaya (India): Tectonics, v. 21, p. 1058–1074, doi:10.1029/2002TC001363.

Wobus, C.W., Hodges, K.V., and Whipple, K.X., 2003, Has focused denudation sustained active thrusting at the Himalayan topographic front?: Geology, v. 31, p. 861–864, doi:10.1130/G19730.1.

Wobus, C.W., Heimsath, A.M., Whipple, K.X., and Hodges, K.V., 2005, Active out-of-sequence thrust faulting in the central Nepalese Himalaya: Nature, v. 434, p. 1008–1011, doi:10.1038/nature03499.

Wobus, C.W., Whipple, K.X., and Hodges, K.V., 2006, Neotectonics of the central Nepalese Himalaya: Constraints from geomorphology, detrital $^{40}Ar/^{39}Ar$ thermochronology, and thermal modeling: Tectonics, v. 25, doi:10.1029/2005TC001935.

Yin, A., 2006, Cenozoic tectonic evolution of the Himalayan orogen as constrained by along-strike variation of structural geometry, exhumation history, and foreland sedimentation: Earth-Science Reviews, v. 76, p. 1–131, doi:10.1016/j.earscirev.2005.05.004.

Yin, A., Harrison, T.M., Ryerson, F.J., Chen, W., Kidd, W.S.F., and Copeland, P., 1994, Tertiary structural evolution of the Gangdese thrust system, southeastern Tibet: Journal of Geophysical Research, v. 99, p. 18175-18201.

Yin, A., Harrison, T.M., Murphy, M.A., Grove, M., Nie, S., Ryerson, F.J., Wang, X.F., and Chen, Z.L., 1999, Tertiary deformation history of southeastern and southwestern Tibet during the Indo-Asian collision: Geological Society of America Bulletin, v. 111, p. 1644–1664, doi:10.1130/0016-7606(1999)111<1644:TDHOSA>2.3.CO;2.

Yin, A., Dubey, C.S., Kelty, T.K., Webb, A.A.G., Harrison, T.M., Chou, C.Y., and Célérier, J., 2010, Geologic correlation of the Himalayan orogen and Indian craton: Part 2. Structural geology, geochronology, and tectonic evolution of the Eastern Himalaya: Geological Society of America Bulletin, v. 122, p. 360–395, doi:10.1130/B26461.1.

Zhang, R., Murphy, M., Lapen, T.J., Sanchez, V., and Heizler, M., 2011, Late Eocene crustal thickening followed by Early–Late Oligocene extension along the India-Asia suture zone: Evidence for cyclicity in the Himalayan orogen: Geosphere, v. 7, p. 1249–1268, doi:10.1130/GES00643.1.